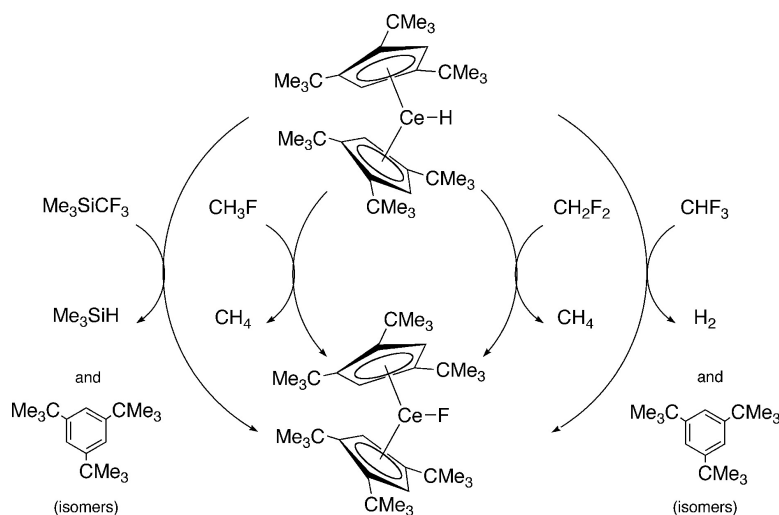


Hydrogen for Fluorine Exchange in CHF by Monomeric [1,2,4-(Me₃C)CH]CeH: Experimental and Computational Studies

Evan L. Werkema, Elsa Messines, Lionel Perrin, Laurent Maron, Odile Eisenstein, and Richard A. Andersen

J. Am. Chem. Soc., **2005**, 127 (21), 7781-7795 • DOI: 10.1021/ja0504800 • Publication Date (Web): 07 May 2005

Downloaded from <http://pubs.acs.org> on March 25, 2009



More About This Article

Additional resources and features associated with this article are available within the HTML version:

- Supporting Information
- Links to the 19 articles that cite this article, as of the time of this article download
- Access to high resolution figures
- Links to articles and content related to this article
- Copyright permission to reproduce figures and/or text from this article

[View the Full Text HTML](#)

Hydrogen for Fluorine Exchange in $\text{CH}_{4-x}\text{F}_x$ by Monomeric $[1,2,4-(\text{Me}_3\text{C})_3\text{C}_5\text{H}_2]_2\text{CeH}$: Experimental and Computational Studies

Evan L. Werkema,[†] Elsa Messines,[‡] Lionel Perrin,[§] Laurent Maron,^{*,‡}
Odile Eisenstein,^{*,§} and Richard A. Andersen^{*,†}

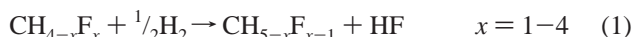
Contribution from the Chemistry Department and Chemical Sciences Division of Lawrence Berkeley National Laboratory, University of California, Berkeley, California 94720, Laboratoire de Physique Quantique, UMR 5626-CNRS, IRSAMC, Université Paul Sabatier, 118 Route de Narbonne, 31064 Toulouse Cedex 04, France, and LSDSMS, (UMR 5636-CNRS), Institut Gerhardt, cc14, Université Montpellier 2, 34095 Montpellier Cedex 5, France

Received January 24, 2005; E-mail: laurent.maron@irsamc.ups-tlse.fr; odile.eisenstein@univ-montp2.fr; raandersen@lbl.gov

Abstract: The monomeric metallocenecerium hydride, $\text{Cp}'_2\text{CeH}$ ($\text{Cp}' = 1,2,4\text{-tri-}t\text{-butylcyclopentadienyl}$), reacts instantaneously with CH_3F , but slower with CH_2F_2 , to give $\text{Cp}'_2\text{CeF}$ and CH_4 in each case, a net H for F exchange reaction. The hydride reacts very slowly with CHF_3 , and not at all with CF_4 , to give $\text{Cp}'_2\text{-CeF}$, H_2 , and 1,2,4- and 1,3,5-tri-*tert*-butylbenzene. The substituted benzenes are postulated to result from trapping of a fluorocarbene fragment derived by α -fluoride abstraction from $\text{Cp}'_2\text{CeCF}_3$. The fluoroalkyl, $\text{Cp}'_2\text{CeCF}_3$, is generated by reaction of $\text{Cp}'_2\text{CeH}$ and Me_3SiCF_3 or by reaction of the metallacycle, $[(\text{Cp}')-(\text{Me}_3\text{C})_2\text{C}_5\text{H}_2\text{C}(\text{Me}_2)\text{CH}_2]\text{Ce}$, with CHF_3 , and its existence is inferred from the products of decomposition, which are $\text{Cp}'_2\text{CeF}$, the isomeric tri-*tert*-butylbenzenes and in the case of Me_3SiCF_3 , Me_3SiH . The fluoroalkyls, $\text{Cp}'_2\text{CeCH}_2\text{F}$ and $\text{Cp}'_2\text{CeCHF}_2$, generated from the metallacycle and CH_3F and CH_2F_2 , respectively, are also inferred by their decomposition products, which are $\text{Cp}'_2\text{CeF}$, CH_2 , and CHF , respectively, which are trapped. DFT(B3PW91) calculations have been carried out to examine several reaction paths that involve CH and CF bond activation. The calculations show that the CH activation by $\text{Cp}'_2\text{CeH}$ proceeds with a low barrier. The carbene ejection and trapping by H_2 is the rate-determining step, and the barrier parallels that found for reaction of H_2 with CH_2 , CHF , and CF_2 . The barrier of the rate-determining step is raised as the number of fluorines increases, while that of the CH activation path is lowered as the number of fluorines increases, which parallels the acidity.

Introduction

The hydrogen for fluorine exchange reaction in fluoromethanes is a thermodynamically favorable transformation. The exchange reaction is exothermic by 20–30 kcal mol⁻¹ because the exchange results in formation of HF, eq 1, in which the bond disruption enthalpy of 135 kcal mol⁻¹ is 30 kcal mol⁻¹ larger than that of H_2 (105 kcal mol⁻¹). The C–F bond dissociation enthalpy (BDE) monotonically decreases on going from CF_4 to CH_3F , the average BDE values of CF_4 , CHF_3 , CH_2F_2 , and CH_3F are 130, 129, 120, and 108 kcal mol⁻¹, respectively, making the reaction more exothermic as the fluorine content decreases. The C–H BDE in the fluoromethanes decreases from 107 to 100 kcal mol⁻¹ in the above series.¹



The exchange does not occur, however, without a catalyst. For example, passing a mixture of CH_3F and H_2 over Pd/C at

240 °C results in a 10% conversion to methane.² The favorable thermodynamics of eq 1 are clearly due to the bond enthalpy of H–F being greater than either the H–H or the C–F bond. Lanthanide fluorides, in general, have average bond enthalpies larger than that of HF, for example, the average bond enthalpy of $\text{CeF}_3(\text{g})$ is 153 kcal mol⁻¹.³ Although the Ce–H bond enthalpy in CeH_3 is unknown, it is likely to be less than that of H–H, as is the case for the metallocenes, $\text{Cp}'_2\text{MH}$; the M–H bond enthalpy is 67 kcal mol⁻¹ in $(\text{Me}_5\text{C}_5)_2\text{LaH}$ or $(\text{Me}_5\text{C}_5)_2\text{-LuH}$ and 80 kcal mol⁻¹ in $(\text{Me}_5\text{C}_5)_2\text{ZrH}_2$,⁴ and the H/F exchange reaction will be exothermic. Bare cationic metal atoms in the gas-phase defluorinate some fluoromethanes. For example, $\text{Ce}^+(\text{g})$ forms $\text{CeF}_2^+(\text{g})$ from CH_3F , but no abstraction is observed from CHF_3 or CF_4 , bracketing the $\text{CeF}^+(\text{g})$ bond enthalpy between 110 and 130 kcal mol⁻¹.⁵

The H/F exchange reactions in halofluoromethanes are of some interest in the biological community because the cobal-

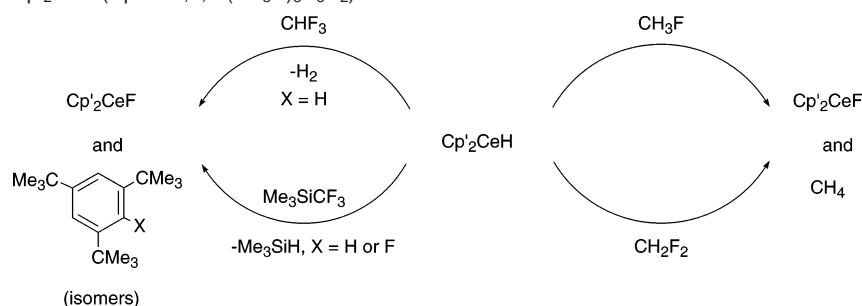
[†] University of California, Berkeley.

[‡] Université Paul Sabatier.

[§] Université Montpellier 2.

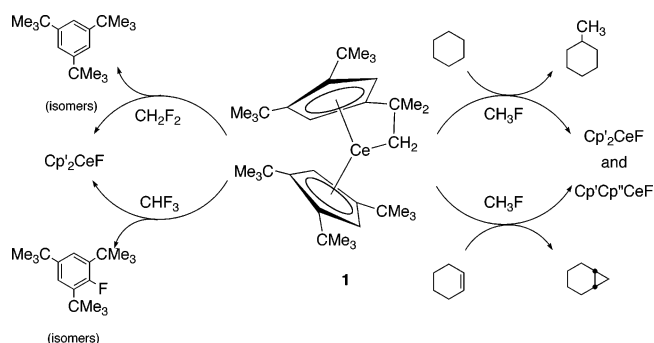
(1) Slayden, S. W.; Liebman, J. F.; Mallard, W. G. In *The Chemistry of Halides, Pseudohalides and Azides*; Supp D2; Patai, S., Rappoport, Z., Eds.; Wiley: Chichester 1995; p 386.

(2) Hudlicky, M. *J. Fluorine Chem.* **1989**, *44*, 345. Lacher, J. R.; Kianpour, A.; Park, J. D. *J. Phys. Chem.* **1956**, *60*, 1454. Larcher, J. R.; Kianpour, A.; Otting, F.; Park, J. D. *Trans Faraday Soc.* **1956**, *52*, 1500.
(3) Pankratz, L. B. "Thermodynamic Properties of Halides, Bulletin 674, Bureau of Mines", 1984.
(4) Nolan, S. P.; Stern, D.; Hedden, D.; Marks, T. J. *ACS Symp. Ser.* **428** **1990**, 159–174. Schock, L. E.; Marks, T. J. *J. Am. Chem. Soc.* **1988**, *110*, 7701.

Scheme 1. Reactions of $\text{Cp}'_2\text{CeH}$ ($\text{Cp}' = 1,2,4\text{-}(\text{Me}_3\text{C})_3\text{C}_5\text{H}_2$) with Fluorocarbons

amines defluorinate them. For example, photolysis of cobalamines in the presence of CHF_2Cl and H_2 yields methane. The mechanism of this reaction is unknown, but a mechanism in which $\alpha\text{-F}$ abstraction from a $(\text{L})\text{CoCHF}_2$ species followed by trapping of the resulting carbene with H_2 has been suggested.⁶ In related experiments, corrinoids catalyze the reduction of, for example, CF_3Cl to CO in the presence of Ti^{III} citrate in water. The mechanism is suggested to involve formation of carbenes that are trapped by water to give CO and HX .⁷ The organometallic chemistry literature contains examples of model systems that relate, in a general way, to the biological ones mentioned. The iridium cation, $(\text{Me}_5\text{C}_5\text{Ir}(\text{PMe}_3)(\text{H}_2\text{O})(\text{C}_2\text{F}_5)^+$, undergoes hydrogenolysis to give CH_2FCF_3 and CH_3CF_3 by a mechanism proposed to proceed by way of an iridium carbene species.⁸ The aqueous acid hydrolysis of $[\text{CF}_3\text{Cr}(\text{OH}_2)_5]^{2+}$ gives $[\text{FCr}(\text{OH}_2)_5]^{2+}$ and CO , a reaction also suggested to involve hydrolysis of a carbene.⁹ Experimental and computational studies of the carbene transfer to various traps have been carried out for RCH_2LiX where X is chloride, bromide, or iodide, the Simmons–Smith reagent RCH_2ZnI , and with ISmCH_2I .¹⁰

Thus, reactions of organometallic compounds can provide model systems that illuminate pathways followed by much more complex molecules. Recently, we developed the synthesis of the monomeric metallocene hydride of cerium, $\text{Cp}'_2\text{CeH}$ where Cp' is 1,2,4-*tert*-butylcyclopentadienyl, and showed that it undergoes H/F exchange reactions with C_6F_6 and $\text{C}_6\text{F}_5\text{H}$.¹¹ The general subject of intermolecular C–F activation has been extensively studied, and several reviews are available, largely within the framework of oxidative addition reactions.¹² Computational studies have shown that the C–F activation may be exothermic but that a high activation barrier is usually observed with late transition metal systems.¹³ In the case of early transition

Scheme 2. Reactions of the Metallocycle **1**, Where $\text{Cp}' = 1,2,4\text{-}(\text{Me}_3\text{C})_3\text{C}_5\text{H}_2$ and $\text{Cp}'' = (\text{Me}_2\text{Et})(\text{Me}_3\text{C})_2\text{C}_5\text{H}_2$, with Fluorocarbons

metals, the activation barrier is generally lower and several cases of H/F exchange have been observed; it appears that the $\text{C}(\text{sp}^2)\text{-F}$ bond is activated more easily than the $\text{C}(\text{sp}^3)\text{-F}$ bond.¹⁴ The reactions of bare metal centers have been analyzed by computational methods, showing that electron transfer as well as oxidative insertion paths are possible.¹⁵ In this paper, we show that $\text{Cp}'_2\text{CeH}$ reacts with hydrofluoromethanes, and we explore the mechanistic pathways by DFT calculations on the model metallocene hydride, Cp_2CeH .

Results and Their Interpretation

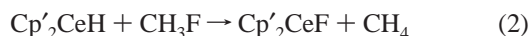
General. The reactions of $\text{Cp}'_2\text{CeH}$ or the metallocycle, **1**, and the fluoromethanes $\text{CH}_{4-x}\text{F}_x$ ($x = 0\text{--}4$), Schemes 1 and 2, are studied by monitoring the changes that occur in the ^1H NMR spectrum in C_6D_6 or C_6D_{12} over time; the *tert*-butyl resonances of the paramagnetic hydride disappear and those of $\text{Cp}'_2\text{CeF}$ appear. The identity of the non-cerium containing products is deduced by the characteristic resonances in their ^1H and ^{19}F NMR spectra. At the end of the reactions, the samples are hydrolyzed (H_2O or D_2O) and examined by GCMS to deduce their identity. In those cases where the reaction is rapid, the

- (5) Cornehl, H. H.; Hornung, G.; Schwarz, H. *J. Am. Chem. Soc.* **1996**, *118*, 9960. Mazurek, U.; Schwarz, H. *Chem. Commun.* **2003**, 1321.
 (6) Penley, M. W.; Brown, D. G.; Wood, J. M. *Biochemistry* **1970**, *9*, 4302.
 (7) Krone, U. E.; Thauer, R. K.; Hogenkamp, H. P. C.; Steinbach, K. *Biochemistry* **1991**, *30*, 2713.
 (8) Hughes, R. P.; Willemsen, S.; Williamson, A.; Zhang, D. *Organometallics* **2002**, *21*, 3085.
 (9) Malik, S. K.; Schmidt, W.; Spreer, L. O. *Inorg. Chem.* **1974**, *13*, 2986. Akhtar, M. J.; Spreer, L. O. *Inorg. Chem.* **1979**, *18*, 3327.
 (10) Boche, G.; Lohrenz, J. C. W. *Chem. Rev.* **2001**, *101*, 697. Masaharu, N.; Atsushi, H.; Eiichi, N. *J. Am. Chem. Soc.* **2003**, *125*, 2341. Fang, W. H.; Phillips, D. L.; Wang, D. Q.; Li, Y. L. *J. Org. Chem.* **2002**, *67*, 154. Zhao, C.; Wang, D.; Phillips, D. L. *J. Am. Chem. Soc.* **2003**, *125*, 15200. Wang, D.; Zhao, C.; Phillips, D. L. *J. Org. Chem.* **2004**, *69*, 5512.
 (11) Maron, L.; Werkema, E. L.; Perrin, L.; Eisenstein, O.; Andersen, R. A. *J. Am. Chem. Soc.* **2005**, *127*, 279.
 (12) Kiplinger, J. L.; Richmond, T. G.; Osterberg, C. E. *Chem. Rev.* **1994**, *94*, 373. Richmond, T. G. *Top. Organomet. Chem.* **1999**, *3*, 243. Burdeniuc, J.; Jedlicka, B.; Crabtree, R. H. *Chem. Ber./Recueil* **1997**, *130*, 145. Murphy, E. F.; Murugavel, R.; Roessky, H. W. *Chem. Rev.* **1997**, *97*, 3425. Alonso, F.; Beletskaya, I. P.; Yus, M. *Chem. Rev.* **2002**, *102*, 4009. Braun, T.; Perutz, R. N. *Chem. Commun.* **2002**, 2749. Jones, W. D. *Dalton Trans.* **2003**, 3991.

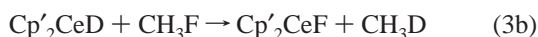
- (13) Su, M. D.; Chu, S.-Y. *J. Am. Chem. Soc.* **1997**, *119*, 10178. Bosque, R.; Fantacci, S.; Clot, E.; Maseras, F.; Eisenstein, O.; Perutz, R. N.; Renkema, K. B.; Caulton, K. G. *J. Am. Chem. Soc.* **1998**, *120*, 12634. Gérard, H.; Davidson, E. R.; Eisenstein, O. *Mol. Phys.* **2002**, *100*, 533. Reinhold, M.; McGrady, J. E.; Perutz, R. N. *J. Am. Chem. Soc.* **2004**, *126*, 5268.
 (14) Edelbach, B. L.; Rahman, A. K. F.; Lachicotte, R.; Jones, W. D. *Organometallics* **1999**, *18*, 3170. Edelbach, B.; Kraft, B. M.; Jones, W. D. *J. Am. Chem. Soc.* **1999**, *121*, 10327. Kraft, B. M.; Lachicotte, R. J.; Jones, W. D. *J. Am. Chem. Soc.* **2000**, *122*, 8559. Kraft, B. M.; Jones, W. D. *J. Organomet. Chem.* **2002**, *658*, 132. Watson, L. A.; Yandulov, D. V.; Caulton, K. G. *J. Am. Chem. Soc.* **2001**, *123*, 603. Yang, H.; Gao, H.; Angelici, R. J. *Organometallics* **1999**, *18*, 2285. Turculet, L.; Tilley, T. D. *Organometallics* **2002**, *21*, 3961. Clot, E.; Mégret, C.; Kraft, B. M.; Eisenstein, O.; Jones, W. D. *J. Am. Chem. Soc.* **2004**, *126*, 5647.
 (15) Harvey, J. N.; Schröder, D.; Koch, W.; Danovich, D.; Shaik, S.; Schwarz, H. *Chem. Phys. Lett.* **1997**, *278*, 391. Chen, Q.; Freiser, B. S. *J. Phys. Chem. A* **1998**, *102*, 3343. Zhang, D.; Liu, C.; Bi, S. *J. Phys. Chem. A* **2002**, *106*, 4153.

reactions are clean and excellent mass balance is observed. In those cases where the reactions are slow, the identity of the major compounds is established, but minor products are not always identified. When feasible, labeling and trapping experiments are used to confirm the spectroscopic results. The synthesis, solution spectroscopy, and solid-state structures of Cp'₂CeH, the starting metallocene, and Cp'₂CeF, the ending metallocene, are known.¹¹

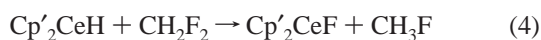
Reactions of Cp'₂CeH and CH_{4-x}F_x; Scheme 1. Exposure of Cp'₂CeH to CH₄ in C₆D₁₂ does not change the appearance of the ¹H NMR spectrum relative to the individual resonances over a month at room temperature. The lack of exchange is not surprising because the Ce–Me bond enthalpy is likely to be less than that of Ce–H, a trend found in f-block and early d-transition metal metallocenes.¹⁶ The reluctance of methane to react with the hydride is fortunate, because exposure of the hydride to CH₃F results in a rapid color change from purple to orange, disappearance of the hydride resonances, and appearance of those due to the fluoride and methane, eq 2.



Methane does not react with the hydride, so the net reaction is a simple H/F exchange. To be certain that the hydride in the methane originates from the cerium hydride, repeating the reaction under an atmosphere of D₂ gives the fluoride and a mixture of CH₄ and CH₃D in approximately equal amounts. This experiment implies that the exchanges symbolized in eqs 3a,b are occurring. No multiple H/D exchange in methane is observed, consistent with the lack of reaction between Cp'₂CeD and methane.

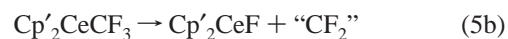
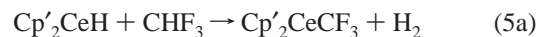


Exposure of Cp'₂CeH to an excess of CH₂F₂ in C₆D₁₂ ultimately gives the same products shown in eq 2, but the rate is much slower, hours rather than seconds. Repeating the reaction in the presence of D₂ gives CH₃D and CH₂D₂ in approximately equal amounts. The HD was not detected presumably because of its low solubility in C₆D₁₂. The labeling result may be rationalized by the net reactions shown in eqs 2 and 4, in which the rate of H/F exchange in eq 4 is slower than that of eq 2. No CH₃F is detected in the ¹H or the ¹⁹F NMR spectrum, consistent with these deductions about the relative rates.



The reaction of CHF₃ is much slower than the other two reactions (eqs 2, 4); weeks rather than hours are required. Although all of the CeH resonances ultimately disappear and Cp'₂CeF is the ultimate cerium containing product formed, no methane is observed in the ¹H NMR spectrum, although a resonance due to dihydrogen appears. Under an atmosphere of either D₂ or CH₄, no deuterated methane or ethane was detected. Several Me₃C-resonances appear in the diamagnetic region of

the ¹H NMR spectrum; these resonances are not due to the isomeric dienes of general formula (Me₃C)₃C₅H₃ formed by hydrolysis from traces of water over the long reaction time, but they were ultimately identified as due to two isomers of tri-*tert*-butylbenzene in the following way. At the end of the reaction, the mixture was hydrolyzed with H₂O (or D₂O) and the hydrolyzate was analyzed by GCMS, which showed two isomers with identical molecular ions whose fragmentation patterns were identified as being those of the isomeric benzenes 1,3,5-(Me₃C)₃C₆H₃ and 1,2,4-(Me₃C)₃C₆H₃. Once the isomers were identified, the resonances due to 1,3,5-(Me₃C)₃C₆H₃ in the ¹H NMR spectrum were compared with those of an authentic specimen. The relative intensity showed that the isomers are present in comparable amounts. The only source of the three *tert*-butyl fragments is the (Me₃C)₃C₅H₂⁻ ring, and the only source of the C₁ fragment is CHF₃. Clearly, the net reaction of CHF₃ is different from that of either CH₂F₂ or CH₃F. The reactions, illustrated in eq 5, may be used to rationalize the identified products. Equation 5a is consistent with the detection of dihydrogen, and eq 5b is consistent with formation of Cp'₂CeF by way of Cp'₂CeCF₃ that is not detected and difluorocarbene that is trapped by a Cp'-ring bound to either Cp'₂CeF or Cp'₂CeH, as illustrated in eqs 5c and 5d. These four equations rationalize the products identified, and they are suggested as a guide to our thinking about the net reaction.



There is literature precedent for carbene insertion into the (Me₃C)₃C₅H₂⁻ ring. Reaction of (Me₃C)₃C₅H₃ and a dihalocarbene generated from CHCl₃ or CHBr₃ and strong base yields the 1,2,4-tri-*tert*-butyl-5-halobenzenes.¹⁷ Although no resonances for Cp'₂CeCF₃ are detected, see later, trifluoromethylmetal species decompose by α-F abstraction to yield CF₂ fragments that are subsequently trapped.¹⁸ Thus, the reaction shown in eq 5b is reasonable, the difluorocarbene is an electrophile and it can add to the different double bonds of the Cp'-ring, and the resulting cerium compounds decompose to isomeric tri-*tert*-butylfluorobenzenes, as illustrated in eq 5c. However, the tri-*tert*-butylfluorobenzenes are not observed; only isomeric tri-*tert*-butylbenzenes are observed. Mixing Cp'₂CeH and the isomeric tri-*tert*-butylfluorobenzenes does not give H/F exchange products; that is, the reaction symbolized in eq 5d does not occur. A possible reason for the absence of tri-*tert*-butylfluorobenzenes is suggested by the following experiments. Mixing Cp'₂CeH and Cp'₂Ce(OSO₂CF₃) instantaneously gives Cp'₂CeF and a new paramagnetic cerium metallocene, thought to be Cp'₂Ce(OSO₂CHF₂), the result of intermolecular H/F exchange analogous to the reaction symbolized in eqs 2 and 4. Mixing Cp'₂CeH with (Cp'-*d*₂₇)₂CeF in C₆D₁₂ instantaneously gives an equilibrium mixture with Cp'₂CeF and (Cp'-*d*₂₇)₂CeH, the net result of intermolecular H/F exchange. Thus, it is reasonable to suggest

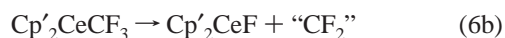
(16) Bruno, J. W.; Marks, T. J.; Morss, L. R. *J. Am. Chem. Soc.* **1983**, *105*, 6824. Bruno, J. W.; Stecher, H. A.; Morss, L. R.; Sonnenberger, D. C.; Marks, T. J. *J. Am. Chem. Soc.* **1986**, *108*, 7275. Martinho Simoes, J. A.; Beauchamp, J. L. *Chem. Rev.* **1990**, *90*, 629.

(17) Dehmow, E. V.; Bollmann, C. *Tetrahedron* **1995**, *51*, 3755.

(18) Banks, R. E. *Fluorocarbons and their Derivatives*, 2nd ed.; MacDonald & Co.: London, 1970; Chapter 4. Seyferth, D. In *Carbenes*; Moss, R. A., Jones, M., Jr., Eds.; Wiley: New York, 1975; Vol. 2, Chapter 3.

that when $\text{Cp}'_2\text{CeCF}_3$ forms (eq 5a), in the presence of $\text{Cp}'_2\text{-CeH}$, rapid intermolecular H/F exchange generates $\text{Cp}'_2\text{CeF}$ and $\text{Cp}'_2\text{CeCHF}_2$, which forms $\text{Cp}'_2\text{CeF}$ and $\text{Cp}'\text{CH}$, the net products observed. Evidence for the decomposition of hypothetical $\text{Cp}'_2\text{-CeCHF}_2$ is provided in the next section.

The sequence of events just outlined demands that $\text{Cp}'_2\text{CeCF}_3$ is formed. Generating or perhaps isolating $\text{Cp}'_2\text{CeCF}_3$ and allowing it to decompose is a crucial experiment, because in absence of this datum, the reactions in eq 5 are without experimental foundation. Generating $\text{Cp}'_2\text{CeCF}_3$ is done in the following manner. Addition of Me_3SiCF_3 to $\text{Cp}'_2\text{CeH}$ in an NMR tube instantly gives resonances due to $\text{Cp}'_2\text{CeF}$, the isomeric tri-*tert*-butylbenzenes and tri-*tert*-butylfluorobenzenes, as well as a resonance due to Me_3SiH . Repeating the experiment with the $[\text{Cp}'\text{-}d_{27}]_2\text{CeD}$ gives Me_3SiD and the isomers of $[(\text{CD}_3)_3\text{C}]_3\text{C}_6\text{H}_2\text{D}$. Trifluoromethyltrimethylsilane in the presence of CsF is a CF_3 transfer reagent for synthesis of $\text{Cp}_2\text{Ti}(\text{CF}_3)(\text{F})$.¹⁹ The net reaction may be written as in eq 6, where the difluorocarbenes are trapped as described above. This set of reactions justifies the speculation about the formation of a trifluoromethyl cerium intermediate, but they just describe the net reaction without mechanistic information.



Exposure of $\text{Cp}'_2\text{CeH}$ to CF_4 in C_6D_{12} for a time period of up to a month does not produce any change in the ^1H NMR spectrum. Thus, CF_4 does not undergo H/F exchange. Although CF_4 is the most stable fluorocarbon known,²⁰ the lack of reaction is kinetic rather than thermodynamic. A very high barrier to H/F exchange of Cp_2LaH and CF_4 is obtained from DFT calculations.²¹ Support for the kinetic stability of CF_4 is derived by noting that the averaged bond dissociation enthalpy of CF_4 is $130 \text{ kcal mol}^{-1}$ while that of $\text{SiF}_4(\text{g})$ is $142 \text{ kcal mol}^{-1}$.³ Mixing $\text{Cp}'_2\text{CeH}$ and SiF_4 generates $\text{Cp}'_2\text{CeF}$ and other unidentified compounds instantaneously, showing that the stronger (Si–F) bond reacts more rapidly than the weaker one (C–F). It is noteworthy that perfluoromethylcyclohexane and $\text{Cp}'_2\text{CeH}$ does indeed produce $\text{Cp}'_2\text{CeF}$, but the reaction time is on the order of a month. Similarly, the PhCF_3 and $\text{Cp}'_2\text{CeH}$ yield resonances due to $\text{Cp}'_2\text{CeF}$ over 3 days; several other cerium containing species were observed in the ^1H NMR spectrum, and these reactions were not studied further.

Summarizing this part, the qualitative results show a large variation in rates of reaction as the H to F ratio changes in the reaction of $\text{Cp}'_2\text{CeH}$ with hydrofluoromethanes. The reactions of $\text{Cp}'_2\text{CeH}$ and CH_3F and CH_2F_2 are clean as only two products are formed, eqs 2 and 4. The reaction of CHF_3 , however, is very slow and produces several products; no methane is detected, but products resulting from difluorocarbene are observed. No mechanistic information is available from these experiments because no intermediates are detected in the NMR experiments. Insight into the mechanisms is explored by DFT calculations described later.

Reaction of the Metallacycle with Hydrofluorocarbons, Scheme 2. The implication of the reaction symbolized by eq 6

is that $\text{Cp}'_2\text{CeCH}_{3-x}\text{F}_x$, $x = 0-3$, in general and $\text{Cp}'_2\text{CeCF}_3$ in particular are unstable relative to $\text{Cp}'_2\text{CeF}$ and a carbene fragment. To learn more about these hypothetical fluoroalkyls and their decomposition pathway, their synthesis was desired. In our previous H/F exchange studies, the metallacycle **1**, in Scheme 2, was shown to react with HC_6F_5 , but not with C_6F_6 , to give the isolable perfluorophenyl derivative, $\text{Cp}'_2\text{Ce}(\text{C}_6\text{F}_5)$. Thus, reactions of the metallacycle with $\text{CH}_{4-x}\text{F}_x$, $x = 0-4$, were explored.

Addition of an excess of CH_4 to the metallacycle in C_6D_{12} does not result in change of appearance of the ^1H NMR spectrum over the period of a month. However, reaction of the metallacycle, in which all of the hydrogens in the CMe_3 groups were exchanged by deuterium, with methane in C_6D_{12} over the course of a week produced some CH_3D . Prolonged exposure gives CH_2D_2 , CHD_3 , and presumably CD_4 . This result implies that the C–H bond of methane can reversibly insert into the Ce–C bond of the metallacycle, a process that is essentially thermoneutral. It is revealing, in this regard, to mention an experiment aimed at the synthesis of $\text{Cp}'_2\text{CeMe}$ from $\text{Cp}'_2\text{CeX}$ ($X = \text{I}$ or O_3SOCF_3) and MeLi in hexanes–ether. Conducting the reaction and workup at room temperature gives a material whose ^1H NMR spectrum (C_6D_6) is identical to that of the metallacycle **1**. When the reaction and workup was repeated at low temperature, the ^1H NMR spectrum showed resonances due to the metallacycle and a pair of Me_3C -resonances in a 2:1 area ratio (see Experimental Section for details). The latter resonances disappear with time as the metallacycle resonances increase in intensity and a resonance due to methane appears. This result is understandable if the Ce–C bonds are assumed to be of comparable strength and the increase of entropy drives the methane elimination reaction. The only alkyl so far isolated is the benzyl, $\text{Cp}'_2\text{CeCH}_2\text{Ph}$, which slowly yields the metallacycle and toluene at room temperature.¹¹

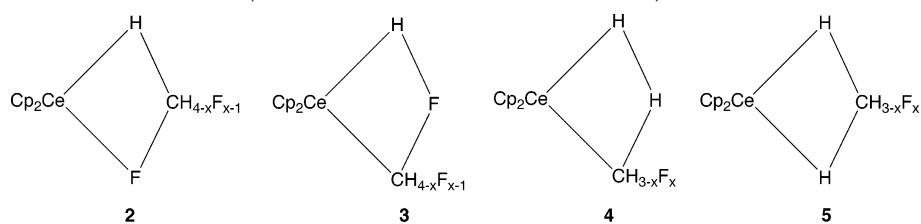
Addition of CH_3F to a solution of the metallacycle in C_6D_{12} in a NMR tube and heating at 60°C over a period of 12 h results in the appearance of resonances due to $\text{Cp}'_2\text{CeF}$ and a set of resonances due to a new cerium metallocene (X) in a 5:1 ratio. The identity of X is established by the following experiments. Repeating the reaction in the presence of cyclohexene showed resonances in the ^1H NMR spectrum due to $\text{Cp}'_2\text{-CeF}$, X , and norcarane (Scheme 2), although the ratio of X to $\text{Cp}'_2\text{CeF}$ is less than in the absence of cyclohexene.²² Repeating the reaction of the metallacycle with CH_3F in C_6D_{12} , without cyclohexene, followed by hydrolysis (H_2O) and analysis of the organic fraction by GCMS shows cyclohexane- d_{12} (solvent), methylcyclohexane- d_{12} , $\text{Cp}'\text{H}$, and a new cyclopentadiene whose m/z value is 14 amu higher than $\text{Cp}'\text{H}$, that is, $\text{Cp}'(\text{CH}_2)\text{H}$. Repeating the above reaction in C_6H_{12} , rather than C_6D_{12} , gives methylcyclohexane in addition to cyclohexane, the solvent. These experiments show that CH_2 is trapped by $\text{C}=\text{C}$ or $\text{C}-\text{H}$

(22) To be sure that cyclohexene does not change the course of the reaction, the perdeuteriometallacycle was exposed to a large excess of cyclohexene in C_6D_{12} . Over the course of a week, 1,2-dideuteriocyclohexene was the only product observed by ^2H NMR spectroscopy. This experiment shows that cyclohexene inserts into the metallacycle to give the metallocene cerium cyclohexenyl derivative and this eliminates cyclohexene- d_1 . Because both olefinic C–H bonds undergo H/D exchange, the process is reversible. The rate of addition is slow, and therefore cyclohexene is present in sufficient excess to act as a trapping reagent. Cyclohexene reacts rapidly with $\text{Cp}'_2\text{-CeH}$ generating the cyclohexenyl derivative that yields the metallacycle and cyclohexane. Under dihydrogen, the metallacycle or $\text{Cp}'_2\text{CeH}$ is a hydrogenation catalyst for cyclohexene. Thus, cyclohexene cannot be used as a carbene trap in reactions of $\text{Cp}'_2\text{CeH}$.

(19) Taw, F. L.; Scott, B. L.; Kiplinger, J. L. *J. Am. Chem. Soc.* **2003**, *125*, 14712.

(20) Banks, R. E.; Tatlow, J. C. *J. Fluorine Chem.* **1986**, *33*, 227.

(21) Perrin, L.; Maron, L.; Eisenstein, O. *Dalton. Trans.* **2003**, 4313.

Scheme 3. Schematic 4c-4e Transition States ($x = 1-4$ for **2** and **3**; $x = 0-3$ for **4** and **5**)

bonds and provides a clue as to the identity of X, because the metallocene rings have C–H bonds. Exposing the perdeuterio-metallacycle to CH_3F in C_6D_{12} showed resonances in the ^2H NMR spectrum due to $(\text{Cp}'\text{-}d_{27})(\text{Cp}'\text{-}d_{26})\text{CeF}$, while the ^1H NMR spectrum contained three new resonances with chemical shifts in the region found for the Me_3C groups in $\text{Cp}'_2\text{CeF}$. Hydrolysis (H_2O) and examination of the hydrolysate by GCMS showed that two cyclopentadienes were present, which were a mixture of the isotopomers $(\text{Cp}'\text{-}d_{26})\text{H}$, $(\text{Cp}'\text{-}d_{27})\text{H}$, and $(\text{Cp}'\text{-}d_{26})(\text{CH}_2)\text{-}(\text{H})$, $(\text{Cp}'\text{-}d_{27})(\text{CH}_2)(\text{H})$, that is, the isotopomers of $\{[(\text{CD}_3)_2(\text{CD}_2\text{-CH}_2\text{D})\text{C}][(\text{CD}_3)_3\text{C}][(\text{CD}_3)_2(\text{CD}_2\text{H})\text{C}]\text{C}_5\text{H}_3\}$. Examination of the ^1H NMR spectrum of the diene shows three single resonances in the $\text{Me}_3\text{C-}$ region for the three possible isotopomers of this diene. This is sufficient evidence to identify X as $[(\text{Me}_2\text{EtC})\text{-}(\text{Me}_3\text{C})_2\text{C}_5\text{H}_2]_2\text{CeF}$, the result of insertion of CH_2 into a C–H bond of the ring substituted CMe_3 group. Thus, C–H bonds of the solvent and the ring substituents trap the CH_2 fragment. However, there is still an unsettling question: photochemical decomposition of CH_2N_2 in the presence of cyclohexene gives norcaradiene and the three isomeric methylcyclohexenes in a ratio of about 2:3.²³ In a later study, singlet CH_2 was found to react with all substrates including C–H bonds of saturated hydrocarbons at diffusion-controlled rates.²⁴ Norcaradiene is the expected reaction product of singlet methylene, but no evidence of insertion into the C–H bonds of cyclohexene is observed in our experiments. A way around the selectivity issue is to postulate that the carbene generated in our studies is not a free carbene, but a carbenoid, that is a methylene, in which the metal and leaving group (F) are still attached to the CH_2 fragment. Carbenoid fragments are electrophiles that react much like free carbenes but show greater selectivity.²⁵ The cerium reaction is therefore related to that observed for various carbenoid precursors such as RHClLiX , the Simmons–Smith reagent, RCHIZnI , and ISMCH_2I .¹⁰ A similar set of experiments with the metallacycle and CH_2F_2 gives $\text{Cp}'_2\text{CeF}$ and the two isomers of *tert*-butylbenzene, or with CHF_3 that gives the isomeric *tri-tert*-butylfluorobenzenes, in the absence of a trapping reagent, Scheme 2. In the presence of cyclohexene, similar results are obtained indicating that cyclohexene is not as good a trap as the substituted-cyclopentadienyl ring. This set of experiments is consistent with the idea that the C–H bond in hydrofluoromethanes inserts into the Ce–C bond of the metallacycle generating a metallocenecerium-fluoroalkyl that is not observed by ^1H NMR spectroscopy, but whose identity is inferred by the products of decomposition. The mechanism of the net reaction shown in Schemes 1 and 2 is explored by DFT calculations in the next section.

Computational Studies

General Considerations. In the calculations, $\text{Cp}'_2\text{CeH}$ is modeled by Cp_2CeH , which changes the steric effects of the metallocene fragment. Because the fluoroalkanes are small

molecules, steric effects are not likely to play an important role in the relative activation barriers. This approach has been used successfully in a number of previous studies.^{11,21,26}

The reactions have a very large thermodynamic driving force because the calculated change in free energies for the net H/F exchange reaction is -77 , -64 , and -57 kcal mol^{-1} for CH_3F , CH_2F_2 , and CHF_3 , respectively, in agreement with the trend in the relative experimental C–F BDE's in the fluoroalkanes. The kinetic barriers and therefore the potential energy surfaces determine the relative rates of reaction and product distribution. Cp_2CeH has a choice of reacting with either a C–F bond or C–H bond of the fluoroalkane $\text{CH}_{4-x}\text{F}_x$, which leads to four types of transition states represented in Scheme 3. The transition state **2** corresponds to C–F activation with the carbon atom at the β position in a 4c-4e metathesis transition state and gives Cp_2CeF and $\text{CH}_{(4-x)+1}\text{F}_{x-1}$ by way of direct H/F exchange. The transition state **3** corresponds to a C–F activation but has the carbon atom located at the α position of the 4c-4e metathesis transition state. It gives an alkyl complex and HF, which form Cp_2CeF and $\text{CH}_{(4-x)+1}\text{F}_{x-1}$ by HF addition to the Ce–C bond. This path is an indirect H/F exchange reaction. The transition state **4** corresponds to C–H activation. Further reaction is required for formation Cp_2CeF and $\text{CH}_{(4-x)+1}\text{F}_{x-1}$. The transition state **5** is a degenerate H/H exchange. The calculated intermediates and transition states will be labeled with x where x is the number of fluorine atoms in the reactant. Many studies of reactivity are discussed on the basis of changes in energy (E) and not of free energy (G), but it is not reasonable to ignore the entropic factor in a bimolecular reaction. There is some discussion about the validity of using entropic values calculated in the gas phase for describing reactions in solution.²⁷ For these reasons, two energy values are given in this paper for all extrema as $\Delta G/\Delta E$ in units of kcal mol^{-1} , where ΔG is the Gibbs energy change relative to a reference and ΔE is the relative energy change with respect to the same reference. In discussing the results, only changes in the free energy are used because ΔG and ΔE values give the same qualitative conclusions.

Reactions with CH_3F . The calculated transition states and intermediates are shown in Figure 1, and the free energy profile is shown in Figure 2.

C–F Activation. A change in free energy of $55.2/47.2$ kcal mol^{-1} is required for crossing transition state **3_{1F}**. This high

(23) von Doering, W. E.; Buttery, R. G.; Laughlin, R. G.; Chaudhuri, N. *J. Am. Chem. Soc.* **1956**, *78*, 3224.

(24) Turro, N. J.; Cha, Y.; Gould, I. R. *J. Am. Chem. Soc.* **1987**, *109*, 2101.

(25) Kirme, W. *Carbene Chemistry*; Academic Press: New York, 1971. Boche, G.; Lohrenz, J. C. W. *Chem. Rev.* **2001**, *101*, 697.

(26) (a) Maron, L.; Eisenstein, O. *J. Am. Chem. Soc.* **2001**, *123*, 1036. (b) Maron, L.; Perrin, L.; Eisenstein, O. *J. Chem. Soc., Dalton Trans.* **2002**, 534. (c) Perrin, L.; Maron, L.; Eisenstein, O. *New J. Chem.* **2004**, *28*, 1255. Niu, S.; Hall, M. B. *Chem. Rev.* **2000**, *100*, 353.

(27) Cooper J.; Ziegler, T. *Inorg. Chem.* **2002**, *41*, 6614. Sakaki, S.; Tatsunori, T.; Michinori, S.; Sugimoto, M. *J. Am. Chem. Soc.* **2004**, *126*, 3332.

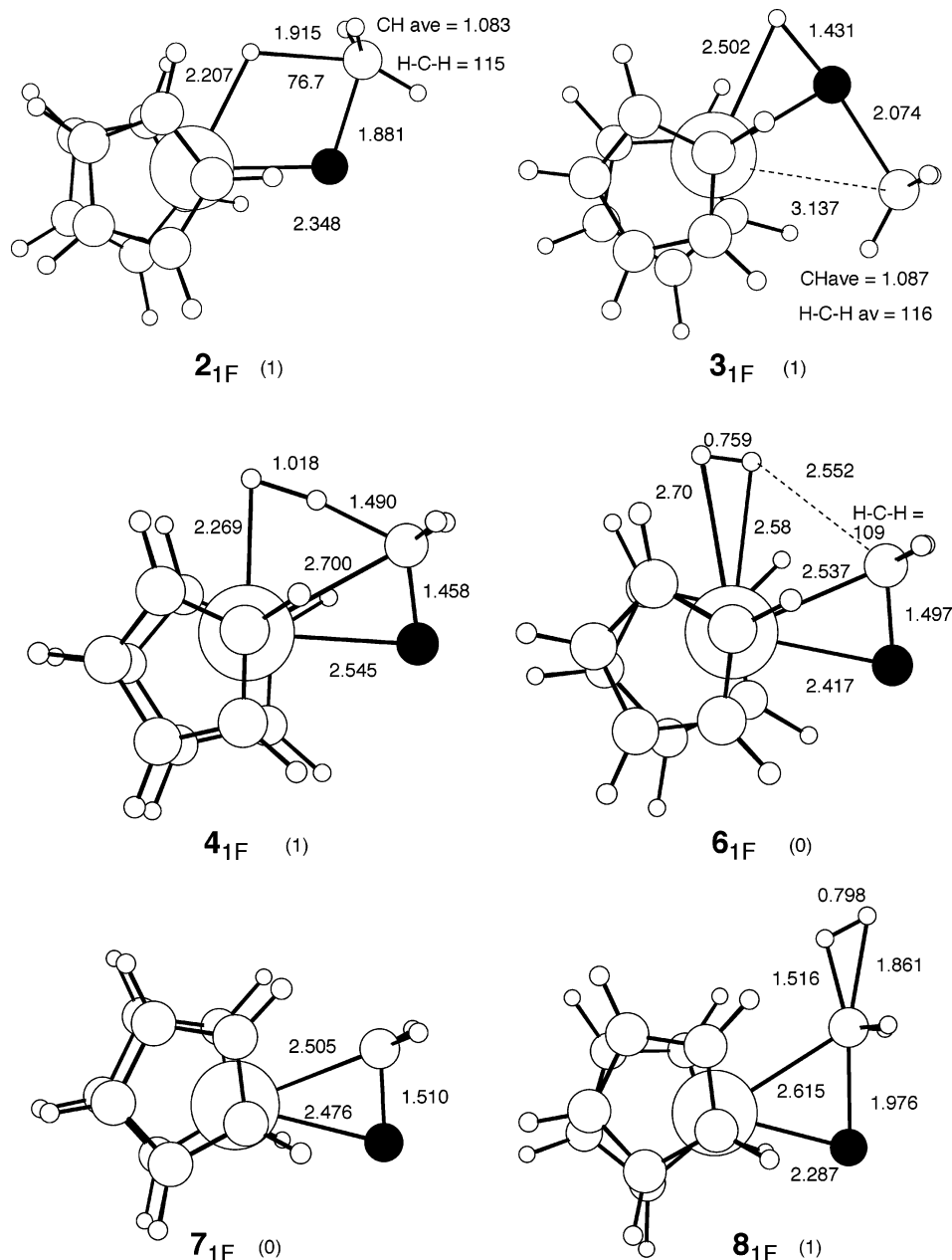


Figure 1. Optimized (B3PW91) structures for the reaction of Cp_2CeH with CH_3F . Distances in angstroms and angles in degrees. The number in parentheses is the number of imaginary frequencies, 0 for a minimum and 1 for a transition state.

value indicates that 3_{1F} is an unlikely transition state for the reaction. The transition state has an unusual geometry: HF is almost formed, while the CH_3 group is far from the metal center. It has been noted that a metathesis transition state in which the electronegative atom is located at the β position in the metathesis transition state is unfavorable because the charge distribution in the 4c-4e transition state accumulates positive charge on the atoms in that position.²¹ Thus, the electronegative fluorine atom will avoid the β -position.

The direct H/F exchange pathway by way of transition state 2_{1F} requires a free energy of activation of 31.1/21.1 kcal mol⁻¹. The direct H/F exchange barrier is considerably lower than 3_{1F} and also lower than the H/H exchange in methane (71.6/62.0 kcal mol⁻¹). The geometry of 2_{1F} shows a slightly pyramidal CH_3 group interacting with H and F. The geometry of the CH_4F^-

fragment is similar to that of a trigonal bipyramid in which the CH_3 group can behave as a turnstile.

C-H Activation. The nonproductive H/H exchange proceeds by way of a transition state 5_{1F} in which the carbon is at the β position in the 4c-4e metathesis transition state; it has a high free energy of activation of 58.7/48.3 kcal mol⁻¹. This calculated barrier is however significantly lower than that calculated for CH_4 (71.6/62.0 kcal mol⁻¹). The C-H activation in which the carbon atom is at the α position proceeds by way of transition state 4_{1F} with a low free energy of activation of 18.0/7.5 kcal mol⁻¹. In 4_{1F} , the carbon atom, the hydrogen atom that is transferred, and the hydride on cerium are essentially collinear (170°) implying that this elementary step is a proton transfer between an anionic alkyl and a hydride, as was previously found in the reaction of Cp_2LnH with H_2 or CH_4 .^{26a,b} In 4_{1F} , the CH_2F

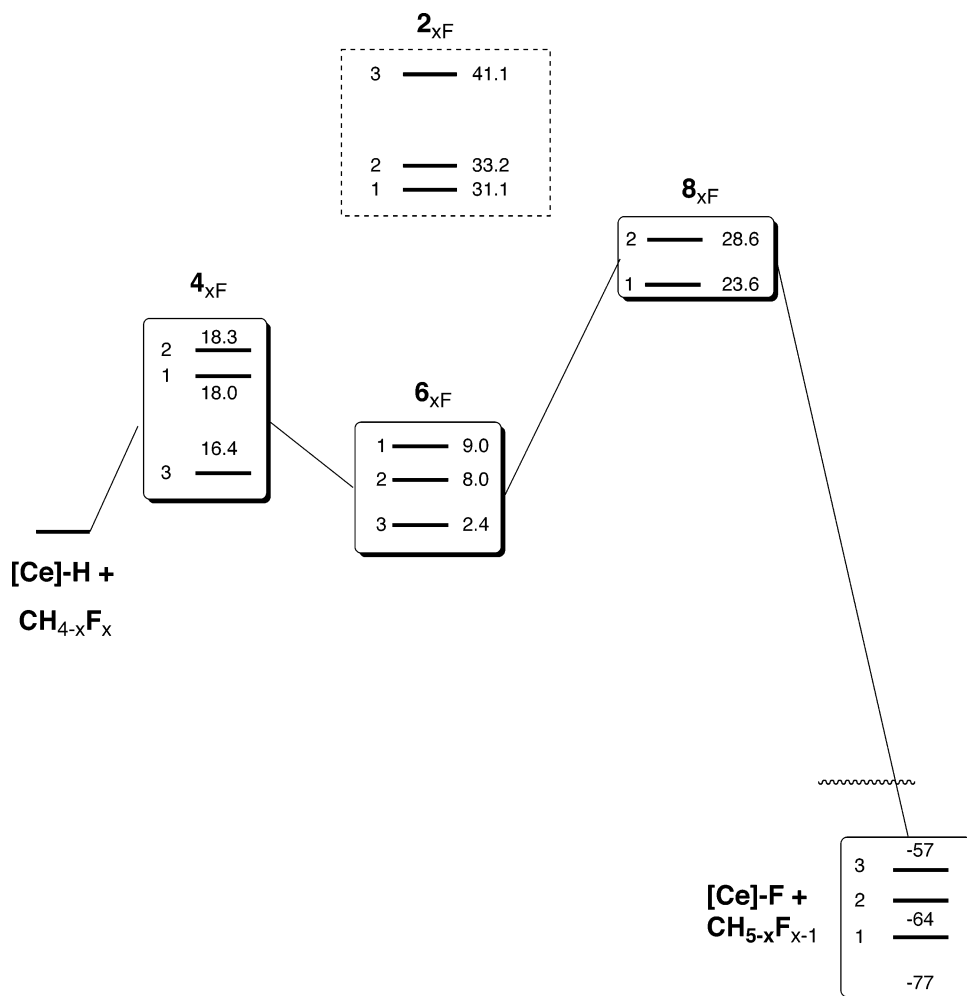


Figure 2. Free energy profile in kcal mol^{-1} for the reactions of Cp_2CeH and $\text{CH}_{4-x}\text{F}_x$ ($x = 1-3$). The value of x is shown on the left at each energy level. The energies in solid boxes correspond to the CH activation, via transition state 4_{xF} , followed by insertion of the carbene into H_2 via transition state 8_{xF} (8_{3F} could not be located). The energies in the dash box correspond to the direct H/F exchange via transition state 2_{xF} .

group is η^2 -bonded to Ce via the C–F bond that is elongated from 1.38 Å in free CH_3F to 1.46 Å in 4_{1F} . Transition state 4_{1F} leads to an adduct, 6_{1F} , between $\text{Cp}_2\text{CeCH}_2\text{F}$ (7_{1F}) and H_2 , which has a free energy of 9.0/–0.2 kcal mol^{-1} relative to separated Cp_2CeH and CH_3F . Dihydrogen is weakly bonded in 6_{1F} ($\Delta E = 0.6 \text{ kcal mol}^{-1}$), and loss of H_2 is entropically driven, $\Delta G = -8.6 \text{ kcal mol}^{-1}$. In $\text{Cp}_2\text{CeCH}_2\text{F}$, 7_{1F} , the C–F bond is stretched to 1.51 Å as Ce–F forms. The Ce–F distance of 2.47 Å compares with 2.16 Å in Cp_2CeF .

The fluoroalkyl is not the final product, so another transformation of the fluoroalkyl is required to account for the end products. Formation of free CH_2 and Cp_2CeF is not possible because the activation energy for this reaction is very high and unfavorable. For example, a separated singlet CH_2 and Cp_2CeF is calculated to be 43.1/59.7 kcal mol^{-1} above the energy of $\text{Cp}_2\text{CeCH}_2\text{F}$. In contrast, insertion of CH_2 into H_2 , with concomitant cleavage of the C–F bond and formation of CH_4 and Cp_2CeF via a transition state shown as 8_{1F} , is only 23.6/14.5 kcal mol^{-1} above the energy of separated reactants Cp_2CeH and CH_3F . At the transition state 8_{1F} , the C–F bond is significantly elongated (1.98 Å) and the shorter distance between C and H_2 is 1.52 Å. The midpoint of H_2 , C, and F are essentially aligned, showing that the p-orbital of CH_2 points toward the leaving fluoride and the incoming H_2 . The interaction

between CH_2 and the metal occurs via the σ orbital of the CH_2 fragment with a relatively short Ce–C distance of 2.6 Å. The H_2 ligand is tilted with respect to the carbene such that the hydrogen atom that is close to the metal is also close to the C atom. This geometry shows that the CH_2 fragment still interacts with the metal and the fluorine atom; that is, it is a carbenoid fragment that behaves as an electrophile.

In the case of CH_3F , two paths with comparable barriers can lead to the observed products as shown by the free energy profile shown in Figure 2. In one path, C–H activation precedes formation of $\text{Cp}_2\text{CeCH}_2\text{F}$ and H_2 . This is followed by a step in which the C–F bond is cleaved and the CH_2 inserts into H_2 . The other path, a direct H/F exchange, has a slightly higher barrier.

Reaction of CH_2F_2 . The replacement of a hydrogen atom by a fluorine in the fluoromethane modifies only slightly the energy pattern calculated for CH_3F (Figure 2). The transition state 3_{2F} for the transfer of F has a free energy of 54.2/45.0 kcal mol^{-1} , which is unfavorable. The free energy (33.2/23.0 kcal mol^{-1}) of the transition state 2_{2F} for the direct H/F exchange is just a little higher than 2_{1F} . The transition state 4_{2F} via C–H activation, forming $\text{Cp}_2\text{CeCF}_2\text{H}$, 7_{2F} , and eliminating H_2 has the lowest activation energy barrier (18.3/8.4 kcal mol^{-1}) for all of the processes considered. The adduct 6_{2F} of H_2 and Cp_2

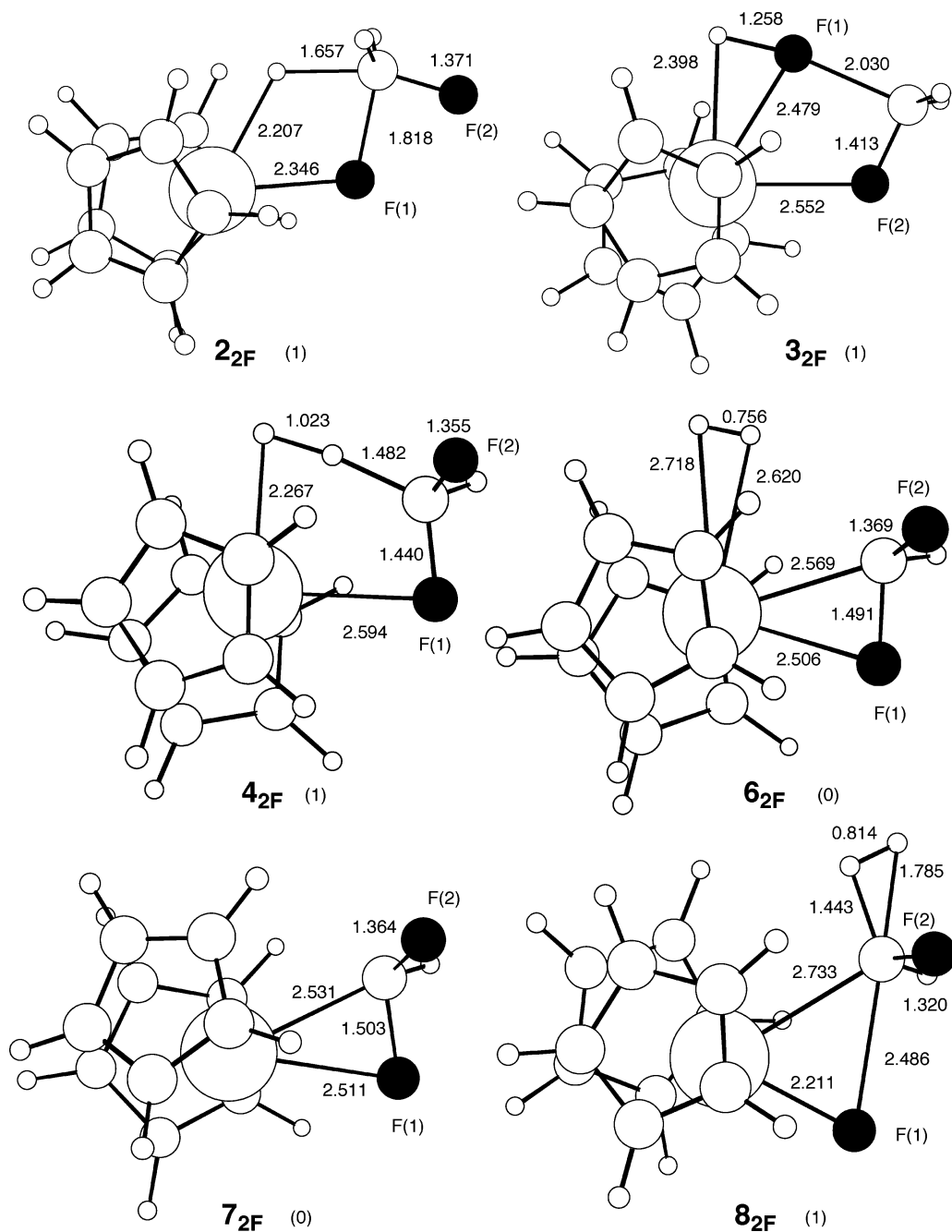


Figure 3. Optimized (B3PW91) structures for the reaction of Cp_2CeH with CH_2F_2 . Distances in angstroms. The number in parentheses is the number of imaginary frequencies, 0 for a minimum and 1 for a transition state.

CeCF_2H has a free energy of $8.0/-1.1$ kcal mol⁻¹ relative to the separated reactants Cp_2CeH and CH_2F_2 . Dissociation of H_2 from **6_{2F}** lowers the free energy by $8.0/0.0$ kcal mol⁻¹. $\text{Cp}_2\text{-CeCF}_2\text{H}$, **7_{2F}**, does not produce free CHF and Cp_2CeF because this transformation is very endoergic ($25.2/41.4$ kcal mol⁻¹). Insertion of CHF into H_2 and the associated formation of $\text{Cp}_2\text{-CeF}$ occurs via transition state **8_{2F}**, which is $28.6/20.0$ kcal mol⁻¹ above the separated reactants Cp_2CeH and CH_2F_2 . Finally, the activation barrier for the degenerate H/H exchange reaction via transition state **5_{2F}** is $62.8/53.4$ kcal mol⁻¹, which is slightly higher than that for CH_3F .

The geometry of the stationary points on the CH_2F_2 potential energy surface is similar to that found for CH_3F as is observed by comparing the structural parameters in Figures 1 and 3. One

of the fluorine atoms of CH_2F_2 , F(1), occupies the site of the unique F of CH_3F in the various stationary points. The other fluorine, F(2), largely influences the electronic environment of the carbon fragment. In **2_{2F}**, F(2) is located on the apical site of a trigonal-based bipyramid formed by CF_2H_3 . The C–F(1) distance is slightly shorter in **7_{2F}** than in **7_{1F}**. In **8_{2F}**, the transition state for insertion of CHF into the H_2 and formation of $\text{Cp}_2\text{-CeF}$, F(2) stabilizes the native carbene $\text{CHF}(2)$ fragment, which results in a longer C–F(1) distance for the bond being cleaved.

Reaction of CHF_3 . The trends in activation energies found in the case of CH_3F and CH_2F_2 are maintained in CHF_3 . The net result of the additional fluorine atoms increases the barrier for all of the transformations except for C–H activation. The transfer of F, via transition state **3_{3F}**, remains high in energy

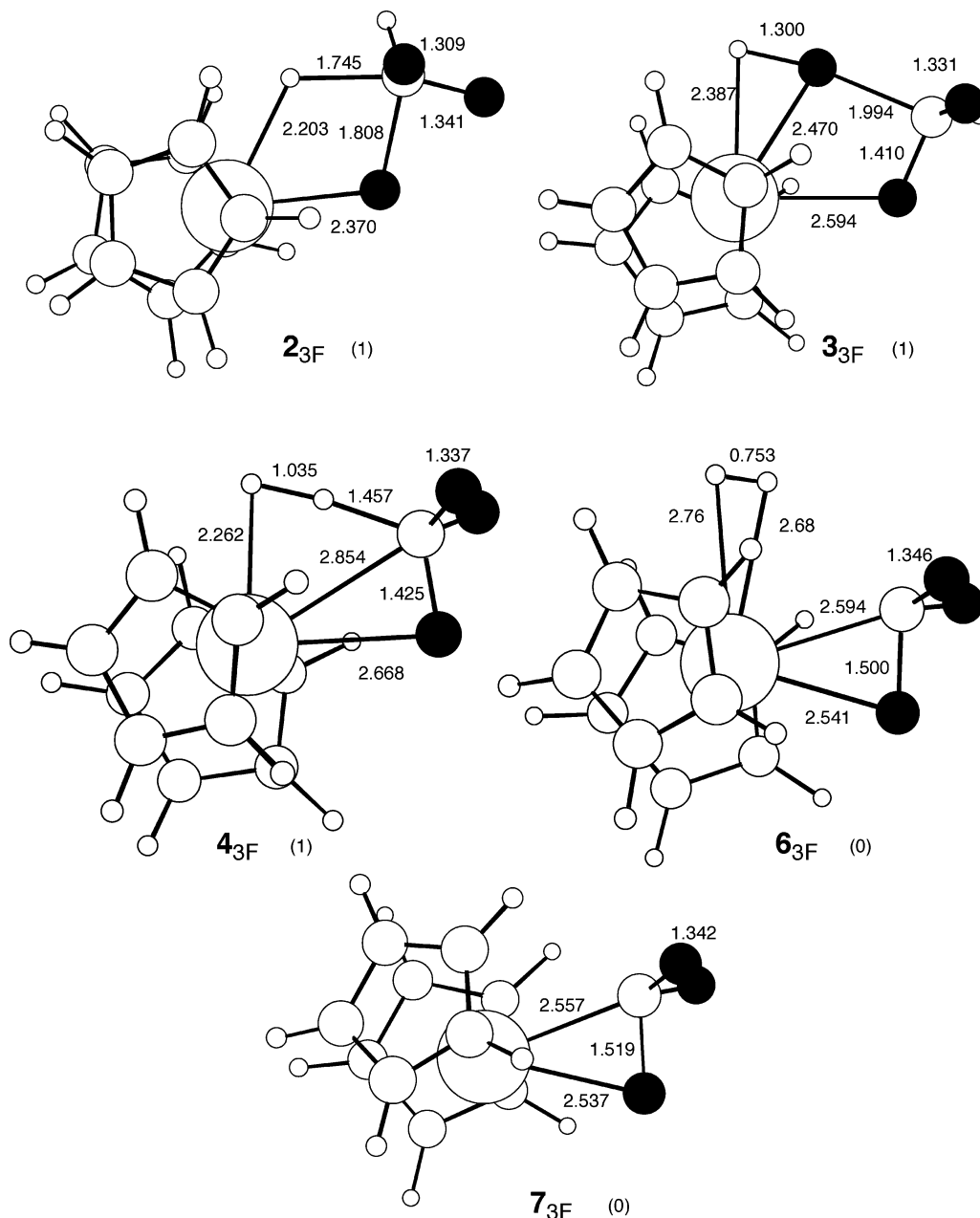


Figure 4. Optimized (B3PW91) structures for the reaction of Cp_2CeH with CHF_3 . Distances in angstroms. The number in parentheses is the number of imaginary frequencies, 0 for a minimum and 1 for a transition state.

(60.0/49.0 kcal mol⁻¹). The activation energy barrier for direct H/F exchange, via transition state $2_{3\text{F}}$, is 41.1/30.0 kcal mol⁻¹. The C–H activation process via transition state $4_{3\text{F}}$ benefits from the increased number of fluorine atoms because the activation energy barrier is only 16.4/6.7 kcal mol⁻¹. The three fluorine atoms increase the acidity of the hydrogen that in turn lowers the barrier for the proton transfer as the hydride forms H_2 . This transition state leads to the formation of an adduct $6_{3\text{F}}$ of H_2 and Cp_2CeCF_3 , whose free energy is 2.4/–6.0 kcal mol⁻¹ relative to separated reactant Cp_2CeH and CHF_3 . Loss of H_2 from $6_{3\text{F}}$ lowers the free energy by 7.7/0.0 kcal mol⁻¹. Cp_2CeCF_3 , $7_{3\text{F}}$, expels CF_2 and forms Cp_2CeF with a change of free energy of 6.3/16.0 kcal mol⁻¹ relative to $7_{3\text{F}}$. The activation energy barrier for the H/H exchange via transition state $5_{3\text{F}}$ is 63.6/51.4 kcal mol⁻¹. The transition state $8_{3\text{F}}$ for insertion of

CF_2 into H_2 and associated cleavage of the C–F bond to form Cp_2CeF and CH_2CF_2 , starting from intermediate $6_{3\text{F}}$, could not be located.

There is no major difference in the geometry of the stationary points as the fluoroalkane is changed from CH_3F to CH_2F_2 to CHF_3 (Figures 1, 3, and 4, respectively). For example, in the transition state $2_{3\text{F}}$, the trigonal bipyramidal fragment CF_3H_2^- has one F near the metal as in CH_3F , one F at the apical site as in CH_2F , and the remaining F is on the equatorial site.

Reaction of CF_4 . The calculated activation barriers for reaction of CF_4 with Cp_2MH have been published,²¹ and some key points that are relevant to the present studies are mentioned here. Only C–F activation is possible, and the activation energies via the transition states $2_{4\text{F}}$ and $3_{4\text{F}}$ are 47.5/32.7 and 57.3/44.5 kcal mol⁻¹, respectively. In accord with the results

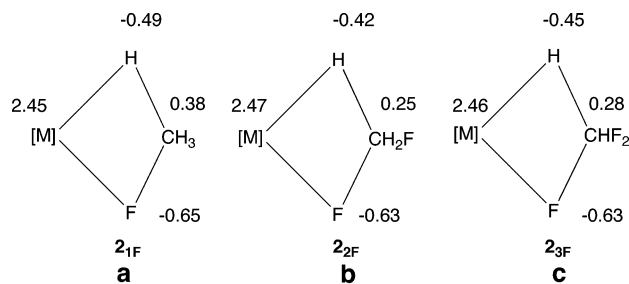


Figure 5. NBO charges on M, H, F, and on the entire group at the β position in the kite-shaped transition state $2_{x\text{F}}$.

on the other fluorinated alkanes described here, $2_{4\text{F}}$ is lower in energy than $3_{4\text{F}}$.

Discussion of the Computational Results. The energy and free energy profiles for the paths going via $2_{x\text{F}}$ (direct H/F exchange) and via $4_{x\text{F}}$ (CH activation) and $8_{x\text{F}}$ (carbene insertion into H_2) are shown in Figure 2. Earlier work has shown that the 4c-4e kite-shaped transition state has a high energy barrier when a carbon atom is located at the site β to the metal center.^{26b,28} The H/H exchange in the reaction of Cp_2CeH with CH_4 has a very high activation energy barrier of 71.6/62.0 kcal mol⁻¹. Introducing one fluorine atom, as in the reaction of Cp_2CeH with CH_3F , lowers the activation energy barrier for the H/F exchange via transition state $2_{1\text{F}}$ by about 40 kcal mol⁻¹ and also lowers the activation energy for H/H exchange via transition state $5_{1\text{F}}$, by around 20 kcal mol⁻¹. Introducing more fluorine atoms, as in the reactions of Cp_2CeH with CH_2F_2 or CHF_3 , raises the activation barriers for the H/F and H/H exchanges as compared to the reaction with CH_3F . It appears that the 4c-4e kite-shaped transition state with a carbon atom at the β site has the lowest energy when only one fluorine is on the carbon center, the H/F exchange being preferred over the H/H exchange. It has been shown that the 4c-4e transition state in the metathesis reaction of the M–H from a metallocene hydride and the C–H bonds of an alkane could be conveniently viewed as the interaction of a Cp_2M^+ cation with an anionic organic fragment formed from the nucleophilic addition of the hydride to the alkane.^{21,26b} Positive and negative charges alternate in the kite-shaped transition state. The NBO analysis at the three transition states $2_{x\text{F}}$ shows that $2_{1\text{F}}$ has the highest negative charge on the hydride and the fluoride and the highest positive charge on the group at the β position (compare a, b, and c in Figure 5).

The bond dissociation energy of H_2 in $6_{x\text{F}}$ is very small, and dissociation of H_2 is favored by the increase in entropy. However, the bond dissociation energy is most likely to be significantly underestimated by the DFT calculations^{29a} despite the fact that B3PW91 was found to perform better than other functionals.^{29b} Calculations with elaborate methods adapted to the calculations of relatively weak interactions cannot be carried out because of the size of the system. It is important to note that H_2 is significantly perturbed by the presence of the $\text{M}^{\delta+}-\text{C}^{\delta-}$ bond because it is strongly positively charged (+0.2 e⁻ on

each H atom), which signals an interaction between the carbon fragment and H_2 .

The transition state for insertion of the carbene into H_2 with synchronous cleavage of C–F(1), $8_{x\text{F}}$, could only be located for the case of CH_3F (insertion of CH_2) and CH_2F_2 (insertion of CHF). The geometry of the carbene $\cdots\text{H}_2$ fragment in the transition state $8_{x\text{F}}$ resembles the geometry of the insertion of the free carbenes into H_2 . The energy barrier increases from $8_{1\text{F}}$ to $8_{2\text{F}}$, which parallels the barriers for insertion of the free carbenes into H_2 .³⁰ The calculated energy barrier at the same level of theory for the reaction of singlet free CH_2 or CHF with H_2 is 4.5 and 8.5 kcal mol⁻¹, respectively. Although these calculations are only indicative of the trends, they mirror the qualitative facts; fluorine deactivates the carbene by stabilizing it. Because the fluoroalkyl cerium group is the source of the carbene, the energy profile for creating a free carbene was calculated. This is highly unfavorable for CH_3F (formation of CH_2), but more favorable with the substituted carbenes. In the case of CHF_3 , formation of CF_2 from $\text{Cp}_2\text{Ce}-\text{CF}_3$ is calculated to be essentially barrierless, and the formation of CF_2 is expected.

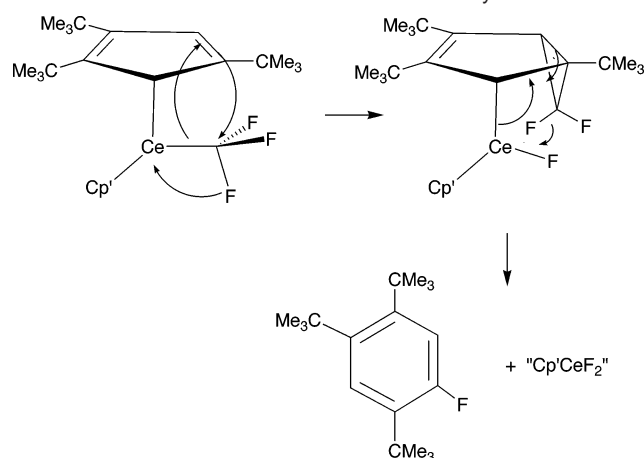
Discussion of the Experimental Results. The calculations suggest that the lowest energy pathway is formation of $\text{Cp}'_2\text{CeCH}_3-x\text{F}_x$, $x = 0-3$, in each case because the intermolecular C–H activation barrier is less than the C–F activation barrier for each of the hydrofluoromethanes studied. This pattern is consistent with the experimental and computational results found for the reaction of $\text{Cp}'_2\text{CeH}$ with C_6F_6 or $\text{C}_6\text{F}_5\text{H}$.¹¹ In the latter set of reactions, the intermediate fluoroaryl, $\text{Cp}'_2\text{CeC}_6\text{F}_5$, was isolated from the reaction of the metallacycle **1** and $\text{C}_6\text{F}_5\text{H}$, and a related strategy was employed for synthesis of the hypothetical $\text{Cp}'_2\text{CeCF}_3$, exposure of metallacycle **1** to CHF_3 . The fluoroalkyl was not detected by ¹H NMR spectroscopy, but $\text{Cp}'_2\text{CeF}$ and the isomeric tri-*tert*-butylfluorobenzenes were observed. The formation of tri-*tert*-butylfluorobenzenes can be rationalized as shown in Scheme 4, in which the $(\text{Me}_3\text{C})_3\text{C}_3\text{H}_2^-$ ligand acts as a trap for CF_2 .¹⁷ An alternative method for generating $\text{Cp}'_2\text{CeCF}_3$ is addition of Me_3SiCF_3 to $\text{Cp}'_2\text{CeH}(\text{D})$, which generates $\text{Me}_3\text{SiH}(\text{D})$, the isomeric tri-*tert*-butylbenzenes, and a small amount of tri-*tert*-butylfluorobenzenes. Our original postulate was that the tri-*tert*-butylfluorobenzenes could undergo H/F exchange, but this is unreasonable because Me_3SiCF_3 reacts instantaneously with $\text{Cp}'_2\text{CeH}$ so the concentration of the hydride is tiny when the fluorobenzenes are formed. This negative inference is shown to be correct by the lack of reaction between the tri-*tert*-butylfluorobenzenes and $\text{Cp}'_2\text{CeH}$. The disappearance pathway was discovered by exposing $(\text{Cp}'\text{-}d_{27})_2\text{CeD}$ to CHF_3 , which generates $(\text{Cp}'\text{-}d_{27})_2\text{CeF}$, and isomeric tri-*tert*-butylbenzenes $[(\text{CD}_3)_3\text{C}]_3\text{C}_6\text{H}_2\text{D}$. This implies that $\text{Cp}'_2\text{CeCF}_3$, which forms slowly in this reaction, undergoes D/F exchange with $\text{Cp}'_2\text{CeD}$ to give $\text{Cp}'_2\text{CeCDF}_2$, and this yields $\text{Cp}'_2\text{CeF}$ and the isomeric deuterio tri-*tert*-butylbenzenes.

The experimental outcome of the reaction of CHF_3 and metallacycle **1**, yielding $\text{Cp}'_2\text{CeCF}_3$, which decomposes to $\text{Cp}'_2\text{-}$

(28) Steigerwald, M. L.; Goddard, W. A., III. *J. Am. Chem. Soc.* **1984**, *106*, 308. Thompson, M. E.; Baxter, S. M.; Bulls, A. R.; Burger, B. J.; Nolan, M. C.; Santarsiero, B. D.; Schaefer, W. P.; Bercaw, J. E. *J. Am. Chem. Soc.* **1987**, *109*, 203. Ziegler, T.; Folga, E. *J. Organomet. Chem.* **1994**, *478*, 57.

(29) (a) Perrin, L.; Maron, L.; Eisenstein, O.; Schwartz, D. J.; Burns, C. J.; Andersen, R. A. *Organometallics* **2003**, *22*, 5447. (b) Wesolowski, T. A.; Parisel, O.; Ellinger, Y.; Weber, J. *J. Phys. Chem. A* **1997**, *101*, 7818.

(30) Dobson, R. C.; Hayes, D. M.; Hoffmann, R. *J. Am. Chem. Soc.* **1971**, *93*, 6188. Bauschlicher, C. W., Jr.; Haber, K.; Schaefer, H. F., III; Bender, C. F. *J. Am. Chem. Soc.* **1977**, *99*, 3610. Rosa, C.; Schlegel, H. B. *J. Am. Chem. Soc.* **1984**, *106*, 5847. Gordon, M. S.; Gano, D. R. *J. Am. Chem. Soc.* **1984**, *106*, 5421. Sironi, M.; Cooper, D. L.; Gerratt, J.; Raimondi, M. *J. Am. Chem. Soc.* **1990**, *112*, 5054. Ignatyev, I. S.; Schaefer, H. F., III. *J. Am. Chem. Soc.* **1997**, *119*, 12306. Jursic, B. J. *J. Mol. Struct. (THEOCHEM)* **1999**, *467*, 103.

Scheme 4. Formation of an Isomer of Tri-*tert*-butylfluorobenzene^a

^a Insertion of the carbene into the other double bond will generate the other isomer. In the case of CHF insertion, only isomeric tri-*tert*-butylbenzenes will form.

CeF and CF₂, is consistent with the calculated barrier. The products derived from the hypothetical intermediates Cp'₂CeCHF₂ or Cp'₂CeCH₂F, formed by reaction of **1** and CH₂F₂ or CH₃F, respectively, are the isomeric tri-*tert*-butylbenzenes and Cp'₂CeF or Cp'₂CeF and [Cp'Cp'']CeF, respectively (Scheme 2). These products may be rationalized by ejection of CHF from Cp'₂CeCHF₂ that is trapped by a C=C bond in the Cp' ligand, but in the case of Cp'₂CeCH₂F, CH₂ is trapped by the C-H bond of the Cp' ligand. However, the products resulting from the reaction of **1** with CH₂F₂ or CH₃F are different from those formed in the reaction of Cp'₂CeH with these two fluoromethanes implying either that Cp'₂CeCH_{3-x}F_x, where $x = 1, 2$, are not formed in the reaction with Cp'₂CeH or that the ejected carbenes are trapped by dihydrogen. No products resulting from a carbene insertion into the Cp' ring are detected in this case. Some circumstantial evidence for dihydrogen acting as a trapping reagent is derived from the products formed in the reaction of the metallacycle and CH₃F, where no dihydrogen is present, because the C-H bonds of solvent or the Me₃C-groups of the cyclopentadienyl ring are traps for the CH₂ fragment. This is consistent with the proposition that the CH₂-fragment rapidly inserts into the C-H or H-H bonds that are in the neighborhood.

Epilogue

The key point that emerges from the calculational study of Cp₂CeH and CH_{4-x}F_x ($x = 1-3$) is that the lowest energy barrier is intermolecular C-H activation forming Cp₂CeCH_{3-x}F_x and H₂. The relative barrier, CH₃F > CH₂F₂ > CHF₃, parallels the acidity because the transition state geometries (Figures 1, 3, and 4) resemble that of a proton-transfer transition state. The cerium alkyl intermediates traverse a higher energy transition state that is associated with large reorganizations of the atoms within the coordination sphere, breaking the C-F bond, making a Ce-F bond and trapping of the carbene fragment. The barrier of the rate-determining step is therefore traced to trapping of the carbenoid fragment, CH₂, CHF, or CF₂. The calculations on the metallocene show that the relative rates of reaction of the carbenoid fragment with H₂ parallel those calculated for insertion of free carbenes into H₂, CH₂ > CHF ≫ CF₂. Thus, the lifetime of the carbene fragments is CH₂ < CHF ≪ CF₂

implying that CH₂ and CHF are trapped by H₂, formed in the C-H activation event. Dihydrogen is therefore an efficient trap in the reaction of Cp'₂CeH with CH₃F and CH₂F₂, because it never leaves the coordination sphere as the products evolve. When H₂ is absent, in the reaction of metallacycle, the C-H and C=C bonds are the only traps that are available. As the lifetime of the CF₂ fragment is longer, it is therefore more selective and it is intramolecularly trapped by insertion into the C=C bond of the cyclopentadienyl ring.

The postulate that the intermolecular C-H activation with lanthanide hydrides precedes the rate-determining step of C-F activation in the fluoromethanes is in agreement with the experimental and calculated results observed in the reaction of aromatic fluorocarbons with the same metallocenes.¹¹ In the latter case, the intermediate Cp'₂CeC₆F₅ was isolated, whereas the analogous intermediate Cp'₂CeCF₃ is not, perhaps because the aromatic C-F bond is stronger than an aliphatic one and the interaction of the C-F bond in the Ce(η^2 -CF₃) group lowers the barrier to Ce-F formation in the latter case, that is, thermodynamic and kinetic differences, respectively. The general reactivity pattern that emerges in these two studies is (i) intermolecular C-H activation is a lower barrier process than C-F activation, (ii) the C-F bond activation is the rate-determining step, and (iii) the net reaction rate (global rate) constant depends on how the intermediates deal with the activation energy barrier on the way to the thermodynamically favored outcome, H/F exchange. Thus, fluorocarbons are inert or relatively inert because of kinetic not thermodynamic factors in *f*- and late *d*- transition metal complexes.¹³ Kinetic factors are the reason for the lack of reaction between Cp'₂CeH and CF₄, whereas Cp'₂CeH does indeed react with C₆F₆ even though the C-F bond is stronger in the latter. Both processes begin by C-F activation, but the change in activation free energy is 30 kcal mol⁻¹ higher for CF₄ than C₆F₆, which is related to the greater ease with which an aromatic ring reorganizes the electronic charges.^{11,21}

Experimental Details

General. Manipulations were performed as previously reported¹¹ except that, unless otherwise noted, samples for GCMS were prepared from NMR reaction samples by adding a drop of H₂O rather than D₂O. The principle elution peaks consisted of free Cp'H and other organic compounds that were identified by their molecular ions and fragmentation patterns, where possible, in concert with their ¹H and ¹⁹F NMR spectra. Fluoromethane gases were obtained from Scott Specialty Gases in 99.99% purity and used as received. The abbreviation Cp' is used for the 1,2,4-tri-*tert*-butylcyclopentadienyl ligand, Cp'-*d*₂₇ is used for the same ligand with all *tert*-butyl groups deuterated, and Cp''H is used for the [Me₂EtC][Me₃C]₂C₅H₂ ligand.

NMR Tube Reaction of CHF₃ and Cp'₂CeH in C₆D₁₂. Cp'₂CeH¹¹ was dissolved in C₆D₁₂ in an NMR tube. The tube was cooled in a liquid nitrogen 2-propanol bath, and the headspace was evacuated and replaced with CHF₃ (1 atm). The tube was warmed to 19 °C and allowed to stand. After 20 min, the ratio of Cp'₂CeH to Cp'₂CeF was 32:1, after 3 days it was 1:3.5, and after 6 days it was 1:18. After 26 days, the solution color had changed from purple to orange, all Cp'₂CeH resonances had disappeared from the ¹H NMR spectrum, and resonances of Cp'₂CeF had appeared. Integration of the *tert*-butyl signal intensities relative to the residual solvent proton signal indicated that slightly less than half an equivalent of Cp'₂CeF had formed relative to the starting material. Resonances due to the two isomers of tri-*tert*-butylbenzene also appeared. GCMS analysis showed two principle components in

addition to Cp'H, with (M)⁺ *m/z* 246 and elution times and fragmentation patterns consistent with isomeric tri-*tert*-butylbenzenes. The isomers were present in approximately a 1:1 ratio and accounted for most of the remainder of the starting material.³¹

NMR Tube Reaction of CHF₃ and (Cp'^{-d₂₇)₂CeD in C₆D₁₂.} Cp'^{-d₂₇}-Ce(CH₂Ph)¹¹ was dissolved in C₆D₆ in an NMR tube. The sample was heated at 60 °C for 13 days to perdeuterate the ring *t*-Bu groups; the sample was taken to dryness and the dark red solid residue redissolved in fresh C₆D₆ after 4 days and again after 8 days. After 13 days, the sample was then taken to dryness, and the dark red solid residue was redissolved in C₆D₁₂. The tube was cooled in a liquid nitrogen 2-propanol bath, and the headspace was evacuated and replaced with D₂ (1 atm). The ratio of the unique *t*-Bu_H to the ring hydrogen resonance in the ¹H NMR spectrum was 1:42. In the ²H NMR spectrum, both *t*-Bu_D resonances were observed, and the ring hydrogen resonance was absent. The tube was cooled in a liquid nitrogen 2-propanol bath, and the headspace was evacuated and replaced with CHF₃ (1 atm). The sample was heated at 60 °C for 1 day, after which time the ring resonance of (Cp'^{-d₂₇)₂CeD had disappeared, the ring resonance of (Cp'^{-d₂₇)₂CeF had appeared in the ¹H NMR spectrum, and resonances consistent with (Cp'^{-d₂₇)₂CeF had appeared in the ²H NMR spectrum. GCMS analysis showed two principal components in addition to (Cp'^{-d₂₇)₂H, with envelopes centered around (M)⁺ *m/z* 274 and elution times consistent with tri-*tert*-butylbenzene-*d*₂₈. The extra deuterium is presumed to come from a D for F exchange between (Cp'^{-d₂₇)₂CeD and an intermediate (Cp'^{-d₂₇)₂CeCF₃; see below.}}}}}}

NMR Tube Reaction of Me₃SiCF₃ and Cp'^{-d₂₇)₂CeH in C₆D₁₂.} Cp'^{-d₂₇}-CeH was dissolved in C₆D₁₂ in an NMR tube. A drop of Me₃SiCF₃ was added. Upon agitation, the purple solution turned orange. The ¹H NMR spectrum showed the presence of Cp'^{-d₂₇)₂CeF, Me₃SiH, and both isomers of tri-*tert*-butylbenzene. The ¹⁹F NMR spectrum contained two new resonances consistent with two isomers of tri-*tert*-butylfluorobenzene. GCMS analysis showed four principal components in addition to Cp'H, two with (M)⁺ *m/z* 246 and elution times consistent with isomeric tri-*tert*-butylbenzenes, and two with (M)⁺ *m/z* 264 consistent with isomeric tri-*tert*-butylfluorobenzenes. The ratio of tri-*tert*-butylbenzenes to tri-*tert*-butylfluorobenzenes was approximately 8:1. The symmetric and asymmetric isomers of tri-*tert*-butylbenzene were present in approximately equal amounts (¹H NMR), while those of tri-*tert*-butylfluorobenzene were present in a 1.5:1 ratio (¹⁹F NMR). Characterization of tri-*tert*-butylfluorobenzene: symmetric isomer, ¹⁹F NMR (C₆D₁₂) δ -111.38 (1F, s), GCMS (M)⁺ *m/z* (calcd, found) 264 (100,-100) 265 (20,22) 266 (2,3); asymmetric isomer, ¹⁹F NMR (C₆D₁₂) δ -95.86 (1F, d, *J*_{H-F} = 16 Hz), GCMS (M)⁺ *m/z* (calcd, found) 264 (100,100) 265 (20,34) 266 (2,7).}

NMR Tube Reaction of Me₃SiCF₃ and (Cp'^{-d₂₇)₂CeD in C₆D₁₂.} Cp'^{-d₂₇}-Ce(CH₂Ph) was dissolved in C₆D₆ in an NMR tube. The sample was heated at 60 °C to perdeuterate the ring *t*-Bu groups. After 4 days, the sample was taken to dryness, and the dark red solid residue was redissolved in C₆D₆. The sample was heated for an additional 4 days, then taken to dryness, and the dark red solid residue was dissolved in C₆D₁₂. The tube was cooled in a liquid nitrogen 2-propanol bath, and the headspace was evacuated and replaced with D₂ (1 atm). The ratio of the unique *t*-Bu_H to the ring hydrogen resonance in the ¹H NMR spectrum was 1:4. In the ²H NMR spectrum, both *t*-Bu_D resonances were observed, and the ring hydrogen resonance was absent. A drop of Me₃SiCF₃ was added, and upon agitation, the solution color changed from purple to orange. The ring resonance of (Cp'^{-d₂₇)₂CeD disappeared, and the ring resonance for (Cp'^{-d₂₇)₂CeF had appeared in the ¹H NMR spectrum. Resonances due to (Cp'^{-d₂₇)₂CeF and Me₃SiD appeared in the ²H NMR spectrum, and resonances due to the two isomers of tri-*tert*-butylfluorobenzene-*d*₂₇ appeared in the ¹⁹F NMR spectrum. The sample was twice taken to dryness, redissolved in C₆H₆, and a small amount of Cp'^{-d₂₇)₂CeH was added. After 30 min, the ¹⁹F NMR spectrum}}}}

remained unchanged, but the ²H NMR spectrum contained resonances consistent with both (Cp'^{-d₂₇)₂CeF and (Cp'^{-d₂₇)₂CeH in a 2:1 ratio, implying that H for F exchange occurred. The ¹H NMR spectrum likewise contained resonances of Cp'^{-d₂₇)₂CeF and Cp'^{-d₂₇)₂CeH in the same ratio. GCMS analysis showed four principal components, in addition to Cp'H/(Cp'^{-d₂₇)₂H, two with envelopes centered around (M)⁺ *m/z* 274, with elution times consistent with the isomeric tri-*tert*-butylbenzenes-*d*₂₈, and two with envelopes centered around (M)⁺ *m/z* 291, with elution times consistent with the isomeric tri-*tert*-butylfluorobenzenes-*d*₂₇. The extra deuterium in the tri-*tert*-butylbenzene is presumed to come from a D-F exchange between the intermediate (Cp'^{-d₂₇)₂CeCF₃ and (Cp'^{-d₂₇)₂CeD, generating (Cp'^{-d₂₇)₂CeCDF₂ and (Cp'^{-d₂₇)₂CeF; see later experiments.}}}}}}}}}

NMR Tube Reaction of CH₂F₂ and Cp'^{-d₂₇)₂CeH in C₆D₆.} Cp'^{-d₂₇}-CeH was dissolved in C₆D₁₂ in an NMR tube. The tube was cooled in a liquid nitrogen 2-propanol bath, and the headspace was evacuated and replaced with CH₂F₂ (1 atm). The tube was warmed to 19 °C and allowed to stand. After 10 min, the ratio of Cp'^{-d₂₇)₂CeH to Cp'^{-d₂₇)₂CeF by ¹H NMR spectroscopy was 10:1, after 20 min it was 5:1, and after 1 h it was 2:1. After 1 day, all of the resonances due to Cp'^{-d₂₇)₂CeH had disappeared and an equivalent amount of Cp'^{-d₂₇)₂CeF had formed along with CH₄. Over the time period of the experiment, the color had turned from purple to orange.}}}}

NMR Tube Reaction of D₂, CH₂F₂, and Cp'^{-d₂₇)₂CeD in C₆D₆.} Cp'^{-d₂₇}-Ce(CH₂Ph) was dissolved in C₆D₆ in an NMR tube. The tube was cooled in a liquid nitrogen 2-propanol bath, and the headspace was evacuated and replaced with D₂. The tube was warmed to 19 °C and shaken vigorously. Analysis by ¹H NMR spectroscopy confirmed the presence of Cp'^{-d₂₇)₂CeD. The tube was cooled in a liquid nitrogen 2-propanol bath, and the headspace was partially evacuated and replaced with CH₂F₂. The sample was stored at 19 °C for 1 day, after which time the solution color had changed from purple to orange. Analysis by ¹H NMR confirmed the absence of Cp'^{-d₂₇)₂CeD and the formation of Cp'^{-d₂₇)₂CeF. In addition, the spectrum contained resonances characteristic of CH₄ and CH₃D in an approximately 1:1 area ratio; a trace of CH₂D₂ but no CHD₃ was observed in the spectrum.}}}

NMR Tube Reaction of D₂, CH₂F₂, and (Cp'^{-d₂₇)₂CeD in C₆D₁₂.} Cp'^{-d₂₇}-Ce(CH₂Ph) was dissolved in C₆D₆ in an NMR tube. The sample was heated at 60 °C for 6 days to perdeuterate the ring *t*-Bu groups. The sample was taken to dryness, and the solid residue was redissolved in fresh C₆D₆ and heated at 60 °C for 2 more days to complete the perdeuteration. Analysis by ¹H and ²H NMR confirmed the presence of (Cp'^{-d₂₇)₂CeC₆D₅.¹¹ The tube was cooled in a liquid nitrogen 2-propanol bath, and the headspace was evacuated and replaced with D₂ (1 atm). The tube was warmed to 19 °C and shaken vigorously. Analysis by ¹H and ²H NMR spectroscopy confirmed the presence of (Cp'^{-d₂₇)₂CeD. The tube was cooled in a liquid nitrogen 2-propanol bath, and the headspace was partially evacuated and replaced with CH₂F₂. The sample was stored at 19 °C for 1 day, after which time the solution color had changed from purple to orange. Analysis by ¹H and ²H NMR spectroscopy confirmed the absence of (Cp'^{-d₂₇)₂CeD and the appearance of (Cp'^{-d₂₇)₂CeF. In addition, the ¹H NMR spectrum contained resonances characteristic of CH₄, CH₃D, and CH₂D₂ in an approximately 1:29:60 area ratio; no CHD₃ was observed.}}}}

NMR Tube Reaction of CH₃F and Cp'^{-d₂₇)₂CeH in C₆D₁₂.} Cp'^{-d₂₇}-CeH was dissolved in C₆D₁₂ in an NMR tube. The tube was cooled in a liquid nitrogen 2-propanol bath, and the headspace was evacuated and replaced with CH₃F (1 atm). Upon warming to room temperature with agitation, the color of the solution changed from purple to orange. The ¹H NMR spectrum showed that the Cp'^{-d₂₇)₂CeH had been quantitatively converted to Cp'^{-d₂₇)₂CeF. The resonance due to CH₄ was observed.}}

NMR Tube Reaction of CH₃F, D₂, and Cp'^{-d₂₇)₂CeH in C₆D₁₂.} Cp'^{-d₂₇}-CeH was dissolved in C₆D₁₂ in an NMR tube. The tube was cooled in a liquid nitrogen 2-propanol bath, and the headspace was evacuated and replaced with D₂ (approximately 0.5 atm) and CH₃F (approximately 0.5 atm). Upon warming to room temperature and agitating the solution,

(31) Künzer, H.; Berger, S. *J. Org. Chem.* **1985**, *50*, 3222.

the color changed from purple to orange. The ^1H NMR spectrum showed that the $\text{Cp}'_2\text{CeH}$ had been quantitatively converted to $\text{Cp}'_2\text{CeF}$. Resonances characteristic of CH_4 and CH_3D had also appeared in approximately equal amounts, but no resonances due to CH_2D_2 were observed.

NMR Tube Reaction of CH_3F and $(\text{Cp}'\text{-}d_{27})_2\text{CeD}$ in C_6D_6 . $\text{Cp}'_2\text{CeH}$ was dissolved in C_6D_6 in an NMR tube. The sample was heated at 60°C to perdeuterate the ring *t*-Bu groups and exchange the hydride with deuterium. After 11 days, the ratio of the unique *t*-Bu_H to the ring hydrogen resonance in the ^1H NMR spectrum had changed from 9:1 to 1:4. The tube was cooled in a liquid nitrogen 2-propanol bath, and the headspace was evacuated and replaced with CH_3F (1 atm). Upon warming to room temperature with agitation, the color of the solution changed from purple to orange. The ring resonance of $(\text{Cp}'\text{-}d_{27})_2\text{CeD}$ had been replaced by that of $(\text{Cp}'\text{-}d_{27})_2\text{CeF}$ in the ^1H NMR spectra, and resonances characteristic of CH_4 and CH_3D had also appeared in an approximately 1:2 area ratio; no CH_2D_2 was observed.

NMR Tube Reaction of CH_4 or CF_4 and $\text{Cp}'_2\text{CeH}$ in C_6D_{12} . $\text{Cp}'_2\text{CeH}$ was dissolved in C_6D_{12} in an NMR tube. The tube was cooled in a liquid nitrogen 2-propanol bath, and the headspace was evacuated and replaced with CH_4 or CF_4 (1 atm). The sample was heated at 60°C for 30 days. No change was observed in the ^1H NMR spectrum.

NMR Tube Reaction of CHF_3 and $\text{Cp}'((\text{Me}_3\text{C})_2\text{C}_5\text{H}_2\text{C}(\text{Me}_2)\text{CH}_2)\text{Ce}$ in C_6D_{12} . $\text{Cp}'_2\text{Ce}(\text{CH}_2\text{Ph})$ was dissolved in C_6D_{12} and heated at 60°C for 12 h, yielding a solution of $\text{Cp}'((\text{Me}_3\text{C})_2\text{C}_5\text{H}_2\text{C}(\text{Me}_2)\text{CH}_2)\text{Ce}$. The tube was cooled in a liquid nitrogen 2-propanol bath, and the headspace was evacuated and replaced with CHF_3 (1 atm). The sample was heated at 60°C for 1 day, by which time the resonances for $\text{Cp}'((\text{Me}_3\text{C})_2\text{C}_5\text{H}_2\text{C}(\text{Me}_2)\text{CH}_2)\text{Ce}$ had disappeared from the ^1H NMR spectrum and resonances of $\text{Cp}'_2\text{CeF}$ and several new diamagnetic products had appeared. Addition of a small amount of $\text{Cp}'_2\text{CeH}$ to the solution did not change the ^{19}F NMR spectrum. GCMS analysis showed two primary components in addition to $\text{Cp}'\text{H}$, both with $(\text{M})^+$ m/z 264, consistent with two isomers of tri-*tert*-butylfluorobenzene, one symmetric and the other asymmetric. The ^{19}F NMR spectrum shows that the isomers are present in an approximately 1.5:1 ratio.

NMR Tube Reaction of CHF_3 , Cyclohexene, and $\text{Cp}'((\text{Me}_3\text{C})_2\text{C}_5\text{H}_2\text{C}(\text{Me}_2)\text{CH}_2)\text{Ce}$ in C_6D_{12} . $\text{Cp}'_2\text{Ce}(\text{CH}_2\text{Ph})$ was dissolved in C_6D_{12} and heated at 60°C for 12 h, yielding a solution of $\text{Cp}'((\text{Me}_3\text{C})_2\text{C}_5\text{H}_2\text{C}(\text{Me}_2)\text{CH}_2)\text{Ce}$. A drop of cyclohexene was added. The tube was cooled in a liquid nitrogen 2-propanol bath, and the headspace was evacuated and replaced with CHF_3 (1 atm). The sample was heated at 60°C for 1 day, by which time the resonances for $\text{Cp}'((\text{Me}_3\text{C})_2\text{C}_5\text{H}_2\text{C}(\text{Me}_2)\text{CH}_2)\text{Ce}$ had disappeared from the ^1H NMR spectrum and resonances from $\text{Cp}'_2\text{CeF}$ and several new diamagnetic products had appeared. The ^{19}F NMR spectrum and GCMS analysis were essentially identical to those from the reaction without cyclohexene present.

NMR Tube Reaction of CHF_3 , 2-Methyl-2-heptene, and $\text{Cp}'((\text{Me}_3\text{C})_2\text{C}_5\text{H}_2\text{C}(\text{Me}_2)\text{CH}_2)\text{Ce}$ in C_6D_{12} . $\text{Cp}'_2\text{Ce}(\text{CH}_2\text{Ph})$ was dissolved in C_6D_{12} and heated at 60°C for 12 h, yielding a solution of $\text{Cp}'((\text{Me}_3\text{C})_2\text{C}_5\text{H}_2\text{C}(\text{Me}_2)\text{CH}_2)\text{Ce}$. A drop of 2-methyl-2-heptene was added. The tube was cooled in a liquid nitrogen 2-propanol bath, and the headspace was evacuated and replaced with CHF_3 (1 atm). The sample was heated at 60°C for 1 day, by which time the resonances for $\text{Cp}'((\text{Me}_3\text{C})_2\text{C}_5\text{H}_2\text{C}(\text{Me}_2)\text{CH}_2)\text{Ce}$ had disappeared from the ^1H NMR spectrum and resonances from $\text{Cp}'_2\text{CeF}$ and several new diamagnetic products had appeared. The ^{19}F NMR spectrum and GCMS analysis were essentially identical to those from the reaction without 2-methyl-2-heptene present.

NMR Tube Reaction of CH_2F_2 and $\text{Cp}'((\text{Me}_3\text{C})_2\text{C}_5\text{H}_2\text{C}(\text{Me}_2)\text{CH}_2)\text{Ce}$ in C_6D_{12} . $\text{Cp}'_2\text{Ce}(\text{CH}_2\text{Ph})$ was dissolved in C_6D_{12} and heated at 60°C for 12 h yielding a solution of $\text{Cp}'((\text{Me}_3\text{C})_2\text{C}_5\text{H}_2\text{C}(\text{Me}_2)\text{CH}_2)\text{Ce}$. The tube was cooled in a liquid nitrogen 2-propanol bath, and the headspace was evacuated and replaced with CH_2F_2 (1 atm). The sample was heated at 60°C for 5 days after which time the resonances of $\text{Cp}'((\text{Me}_3\text{C})_2\text{C}_5\text{H}_2\text{C}(\text{Me}_2)\text{CH}_2)\text{Ce}$ had disappeared from the ^1H NMR

spectrum. Resonances due to $\text{Cp}'_2\text{CeF}$ and both isomers of tri-*tert*-butylbenzene had appeared in the spectrum. The presence of both isomers was confirmed by GCMS analysis.

NMR Tube Reaction of CH_3F and $\text{Cp}'((\text{Me}_3\text{C})_2\text{C}_5\text{H}_2\text{C}(\text{Me}_2)\text{CH}_2)\text{Ce}$ in C_6D_{12} . $\text{Cp}'_2\text{Ce}(\text{CH}_2\text{Ph})$ was dissolved in C_6D_{12} and heated at 60°C for 12 h yielding a solution of $\text{Cp}'((\text{Me}_3\text{C})_2\text{C}_5\text{H}_2\text{C}(\text{Me}_2)\text{CH}_2)\text{Ce}$. The tube was cooled in a liquid nitrogen 2-propanol bath, and the headspace was evacuated and replaced with CH_3F (1 atm). The sample was heated at 60°C for 12 h after which time the resonances of $\text{Cp}'((\text{Me}_3\text{C})_2\text{C}_5\text{H}_2\text{C}(\text{Me}_2)\text{CH}_2)\text{Ce}$ had disappeared from the ^1H NMR spectrum. Resonances for $\text{Cp}'_2\text{CeF}$ had appeared, as well as a set of new paramagnetic resonances, presumably due to a new metallocene cerium fluoride. GCMS analysis showed the formation of methylcyclohexane-*d*₁₂, $\text{Cp}'\text{H}$, and a new compound with $(\text{M})^+$ m/z 248, $\text{Cp}'\text{H}+\text{CH}_2$. When the experiment was repeated and D_2O was used to prepare the GCMS sample instead of H_2O , the molecular ion of the new species was m/z 249. The new metallocenes were further identified as described in the next experiment.

NMR Tube Reaction of CH_3F and $(\text{Cp}'\text{-}d_{27})\{[\text{C}(\text{CD}_3)_3]_2\text{C}_5\text{H}_2\text{C}(\text{CD}_3)_2\text{CD}_2\}\text{Ce}$ in C_6D_{12} . $\text{Cp}'_2\text{Ce}(\text{CH}_2\text{Ph})$ was dissolved in C_6D_6 and heated at 60°C for 4 days to perdeuterate the ring *tert*-butyl groups. The sample was taken to dryness, and the solid residue was redissolved in fresh C_6D_6 . The sample was heated for an additional 7 days, then taken to dryness, and the solid residue was redissolved in C_6D_{12} . The sample was heated at 60°C for 1 day, yielding a solution of $(\text{Cp}'\text{-}d_{27})\{[\text{C}(\text{CD}_3)_3]_2\text{C}_5\text{H}_2\text{C}(\text{CD}_3)_2\text{CD}_2\}\text{Ce}$. The tube was cooled in a liquid nitrogen 2-propanol bath, and the headspace was evacuated and replaced with CH_3F (1 atm). The sample was heated at 60°C for 2 days, after which time the resonances of $(\text{Cp}'\text{-}d_{27})\{[\text{C}(\text{CD}_3)_3]_2\text{C}_5\text{H}_2\text{C}(\text{CD}_3)_2\text{CD}_2\}\text{Ce}$ had disappeared from the ^1H and ^2H NMR spectra. Resonances for $(\text{Cp}'\text{-}d_{27})_2\text{CeF}$ had appeared in the ^2H NMR spectrum, as well as hints of the signals with chemical shifts similar those in the ^1H NMR spectrum of the unlabeled, unknown metallocenes from the previous experiment. The ^1H NMR spectrum contained three new resonances due to the three isotopomers arising from the insertion of CH_2 into a C–D bond in $(\text{Cp}'\text{-}d_{27})_2\text{CeF}$. A drop of H_2O was added, and the sample was vigorously shaken. After 10 min, the solution was dried and filtered. The filtrate was added to a new NMR tube and heated at 60°C for 1 day to isomerize the substituted cyclopentadienes. The ^1H NMR spectrum contained three single resonances attributed to the three isotopomers of $(\text{Cp}'\text{-}d_{27})\text{H}$. GCMS analysis showed one major component in addition to $(\text{Cp}'\text{-}d_{27})\text{H}$ (envelope centered around $(\text{M})^+$ m/z 260), with an envelope centered around $(\text{M})^+$ m/z 274. Characterization of the new metallocenes: ^1H NMR (C_6D_{12}) δ -0.100 (2H, $\nu_{1/2} = 20$ Hz), -2.794 (2H, $\nu_{1/2} = 20$ Hz), -6.129 (2H, $\nu_{1/2} = 20$ Hz). Characterization of $\text{Cp}'\text{H}\text{-}d_{27}$: ^1H NMR (C_6D_{12}) δ 1.19 (2H, s), 1.07 (2H, s), 1.00 (2H, s).

NMR Tube Reaction of CH_3F and $\text{Cp}'((\text{Me}_3\text{C})_2\text{C}_5\text{H}_2\text{C}(\text{Me}_2)\text{CH}_2)\text{Ce}$ in C_6H_{12} . $\text{Cp}'_2\text{Ce}(\text{CH}_2\text{Ph})$ was dissolved in C_6H_{12} and heated at 60°C for 12 h yielding a solution of $\text{Cp}'((\text{Me}_3\text{C})_2\text{C}_5\text{H}_2\text{C}(\text{Me}_2)\text{CH}_2)\text{Ce}$. The tube was cooled in a liquid nitrogen 2-propanol bath, and the headspace was evacuated and replaced with CH_3F (1 atm). The sample was heated at 60°C for 12 h. GCMS analysis showed the formation of methylcyclohexane, $\text{Cp}'\text{H}$, and $\text{Cp}'\text{H}$ in addition to solvent cyclohexane.

NMR Tube Reaction of CH_3F , CH_4 , and $\text{Cp}'((\text{Me}_3\text{C})_2\text{C}_5\text{H}_2\text{C}(\text{Me}_2)\text{CH}_2)\text{Ce}$ in C_6D_{12} . $\text{Cp}'_2\text{Ce}(\text{CH}_2\text{Ph})$ was dissolved in C_6D_{12} and heated at 60°C for 12 h yielding a solution of $\text{Cp}'((\text{Me}_3\text{C})_2\text{C}_5\text{H}_2\text{C}(\text{Me}_2)\text{CH}_2)\text{Ce}$. The tube was cooled in a liquid nitrogen 2-propanol bath, and the headspace was evacuated and replaced with CH_4 (0.5 atm) and CH_3F (0.5 atm). The sample was heated at 60°C for 12 h after which time the resonances of $\text{Cp}'((\text{Me}_3\text{C})_2\text{C}_5\text{H}_2\text{C}(\text{Me}_2)\text{CH}_2)\text{Ce}$ had disappeared from the ^1H NMR spectrum. The spectrum contained the same resonances as that of the reaction in the absence of CH_4 .

NMR Tube Reaction of CH_3F , Cyclohexene, and $\text{Cp}'((\text{Me}_3\text{C})_2\text{C}_5\text{H}_2\text{C}(\text{Me}_2)\text{CH}_2)\text{Ce}$ in C_6D_{12} . $\text{Cp}'_2\text{Ce}(\text{CH}_2\text{Ph})$ was dissolved in C_6D_{12} and heated at 60°C for 12 h yielding a solution of $\text{Cp}'((\text{Me}_3\text{C})_2\text{C}_5\text{H}_2\text{C}(\text{Me}_2)\text{CH}_2)\text{Ce}$.

(Me₂)CH₂)Ce. A drop of cyclohexene was added. The tube was cooled in a liquid nitrogen 2-propanol bath, and the headspace was evacuated and replaced with CH₃F (1 atm). The sample was heated at 60 °C for 12 h after which time the resonances of Cp'((Me₃C)₂C₅H₂C(Me₂)CH₂)Ce had disappeared from the ¹H NMR spectrum. Resonances due to Cp'₂CeF had appeared in the ¹H NMR spectrum along with bicyclo-[4.1.0]-heptane (norcarane) and a small amount of the unknown metallocene observed previously. GCMS analysis showed the presence of norcarane, Cp'H, and Cp''H; no methylcyclohexane or methylcyclohexenes were observed.

NMR Tube Reaction of Cyclohexene and Cp'₂CeH in C₆D₆. Cp'₂CeH was dissolved in C₆D₁₂ in an NMR tube, and a drop of cyclohexene (an excess) was added. Within 20 min, resonances due to Cp'₂CeH had disappeared from the ¹H NMR spectrum and resonances of cyclohexane and Cp'((Me₃C)₂C₅H₂C(Me₂)CH₂)Ce had appeared.

NMR Tube Reaction of Cyclohexene and Cp'((Me₃C)₂C₅H₂C(Me₂)CH₂)Ce in C₆D₁₂. Cp'₂Ce(CH₂Ph) was dissolved in C₆D₁₂ and heated at 60 °C for 12 h yielding a solution of Cp'((Me₃C)₂C₅H₂C(Me₂)CH₂)Ce. A drop of cyclohexene was added. After 1 h, a new pair of resonances in a 2:1 area ratio had appeared in the ¹H NMR spectrum. The new product was not further characterized, although it is presumably Cp'₂Ce(cyclohexenyl).

NMR Tube Reaction of Cyclohexene and (Cp'-d₂₇)[C(CD₃)₃]₂C₅H₂[C(CD₃)₂CD₂]₂Ce in C₆D₁₂. Cp'₂Ce(CH₂Ph) was dissolved in C₆D₆ and heated at 60 °C for 4 days to perdeuterate the ring *tert*-butyl groups. The sample was taken to dryness, and the solid residue was redissolved in fresh C₆D₆. The sample was heated for an additional 4 days, then taken to dryness, and the solid residue was redissolved in C₆D₁₂. The sample was heated at 60 °C for 1 day, yielding a solution of (Cp'-d₂₇)[C(CD₃)₃]₂C₅H₂[C(CD₃)₂CD₂]₂Ce. A drop of cyclohexene was added, and the sample was heated at 60 °C. After 1 day, a resonance at 5.63 ppm had appeared in the ²H NMR spectrum, indicating that the protons on the sp²-carbons of cyclohexene were being exchanged for deuterium. The sample was heated at 60 °C for 30 days, over which time this signal increased in intensity 10-fold. No resonances suggesting H for D exchange on the sp³ carbons of cyclohexene could be distinguished from the C₆D₁₂ solvent signal. GCMS analysis showed that cyclohexene was present in large excess, as the molecular ion at (M)⁺ *m/z* 82 was present; in addition, the envelope for the (Cp'-d_{27-x})H centered around *m/z* 247 was also observed.

NMR Tube Reaction of C₇F₁₄ and Cp'₂CeH in C₆D₁₂. Cp'₂CeH was dissolved in C₆D₁₂ in an NMR tube, and a drop of perfluoromethylcyclohexane was added. The sample was stored at ambient temperature for 5 days, by which time resonances of Cp'₂CeF had appeared in the ¹H NMR spectrum. The ratio of Cp'₂CeF to residual Cp'₂CeH was 3:1. After 22 additional days at ambient temperature, only resonances due to Cp'₂CeF were observed in the ¹H NMR spectrum. Identification of the other organic compounds was not pursued.

NMR Tube Reaction of C₆H₅CF₃ and Cp'((Me₃C)₂C₅H₂C(Me₂)CH₂) in C₆D₁₂. Cp'₂Ce(CH₂Ph) was dissolved in C₆D₁₂ and heated at 60 °C for 12 h yielding a solution of Cp'((Me₃C)₂C₅H₂C(Me₂)CH₂)Ce. A drop of C₆H₅CF₃ was added, and the solution was stored at room temperature for 24 h, yielding a red solution. The ¹H NMR spectrum contained resonances for Cp'((Me₃C)₂C₅H₂C(Me₂)CH₂)Ce, a small amount of Cp'₂CeF, and two new paramagnetic species with nearly coincident *tert*-butyl resonances in 2:1 ratios. The ratio of products was not significantly changed by heating the solution for 4 days at 60 °C. The new species were not characterized.

NMR Tube Reaction of C₆H₅CF₃ and Cp'₂CeH in C₆D₁₂. Cp'₂CeH was dissolved in C₆D₁₂ in an NMR tube, and a drop of C₆H₅CF₃ was added. The solution was stored at room temperature for 3 days, by which time the solution color had changed from purple to orange. The ¹H NMR spectrum contained resonances for Cp'₂CeF and the same two new organometallic species observed in the reaction of Cp'-

((Me₃C)₂C₅H₂C(Me₂)CH₂)Ce and C₆H₅CF₃. The ratio of Cp'₂CeF to the new species was 7:1.

Reaction of SiF₄ and Cp'₂CeH. Cp'₂CeH (250 mg, 0.41 mmol) was dissolved in pentane (10 mL). The headspace was evacuated and replaced with SiF₄ (1 atm). The purple solution immediately turned orange, then cloudy and yellow as copious precipitate formed. The ¹H NMR spectrum of the crude product contained four resonances from paramagnetic compounds in a 1:2.5:3.5:3.5 area ratio. The suspension was taken to dryness, and the solid residue was dissolved in 15 mL of toluene. The volume of the solution was reduced until precipitation occurred, warmed to dissolve the precipitate, and then cooled to -15 °C, giving a yellow powder. The ¹H NMR spectrum revealed the same four resonances as the crude product and resonances due to Cp'₂CeF. In an NMR tube, a dilute solution of Cp'₂CeF in C₆D₆ was cooled in a liquid nitrogen 2-propanol bath, and the headspace was evacuated and replaced with SiF₄ (1 atm). The tube was warmed to 19 °C and shaken vigorously. The orange solution turned yellow. The ¹H NMR spectrum was identical to that of the crude product of the reaction of Cp'₂CeH and SiF₄.

Reaction of Cp'₂CeOSO₂CF₃ and CH₃Li. Cp'₂CeOSO₂CF₃ (1 g, 1.3 mmol) was dissolved in 20 mL of diethyl ether and chilled in a liquid nitrogen/2-propanol bath. CH₃Li (1.8 mL of a 0.7 M solution in diethyl ether, 1.3 mmol) was added via syringe. The yellow solution immediately turned red and became cloudy after 10 min. An aliquot was removed and taken to dryness for quick analysis by ¹H NMR spectroscopy. The spectrum of the aliquot showed two new resonances [¹H NMR (C₆D₆): δ -2.31 (36H, ν_{1/2} = 10 Hz), -12.7 (18H, ν_{1/2} = 16 Hz)], possibly due to Cp'₂CeCH₃, as well as resonances due to Cp'-((Me₃C)₂C₅H₂C(Me₂)CH₂)Ce. The latter resonances increased at the expense of the former over time.

NMR Tube Reaction of Cp'₂CeOSO₂CF₃ and Cp'₂CeH in C₆D₆. Approximately equimolar amounts of Cp'₂CeOSO₂CF₃ and Cp'₂CeH were dissolved in C₆D₆ in an NMR tube. The brown solution was stored at room temperature for 1 day. The ¹H NMR spectrum showed the presence of Cp'₂CeF, some residual Cp'₂CeOSO₂CF₃, and a new organocerium species with *tert*-butyl resonances in a 2:1 ratio. The ratio of Cp'₂CeF to the new species was 1:1. The new species is presumed to be Cp'₂CeOSO₂CHF₂, but due to the unavailability of difluoromethanesulfonic acid, it was not possible to synthesize this material independently.

Computational Studies

Computational Details. The Stuttgart–Dresden–Bonn Relativistic large Effective Core Potential (RECP)³² has been used to represent the inner shells of Ce. The associated basis set augmented by an *f* polarization function (α = 1.000) has been used to represent the valence orbitals. *F* has also been represented by the RECP³³ with the associated basis set augmented by two contracted *d* polarization Gaussian functions (α₁ = 3.3505(0.357851), α₂ = 0.9924(0.795561)).³⁴ C and H have been represented by an all-electron 6-31G(d, p) basis set.³⁵ Calculations have been carried out at the DFT(B3PW91) level³⁶ with Gaussian 98.³⁷ The nature of the extrema (minimum or transition state) has been established with analytical frequencies calculations, and the intrinsic reaction coordinate (IRC) has been followed to confirm that transition states connect to reactants and products. The zero point energy (ZPE) and entropic contribution have been estimated within the harmonic potential

(32) Dolg, M.; Stoll, H.; Savin, A.; Preuss, H. *Theor. Chim. Acta* **1989**, *75*, 173. Dolg, M.; Stoll, H.; Preuss, H. *Theor. Chim. Acta* **1993**, *85*, 441.

(33) Igel-Mann, H.; Stoll, H.; Preuss, H. *Mol. Phys.* **1988**, *65*, 1321.

(34) Maron, L.; Teichteil, C. *Chem. Phys.* **1998**, *237*, 105.

(35) Hariharan, P. C.; Pople, J. A. *Theor. Chim. Acta* **1973**, *28*, 213.

(36) Perdew, J. J. P.; Wang, Y. *Phys. Rev. B* **1992**, *82*, 284. Becke, A. D. *J. Chem. Phys.* **1993**, *98*, 5648. Burke, K.; Perdew, J. P.; Yang, W. In *Electronic Density Functional Theory: Recent Progress and New Directions*; Dobson, J. F., Vignale, G., Das, M. P., Eds.; Plenum: New York, 1998.

(37) Pople J. A.; et al. *Gaussian 98*, revision A.9; Gaussian, Inc.: Pittsburgh, PA, 1998.

approximation. The Gibbs free energy, G , was calculated for $T = 298.15$ K. The NBO analysis³⁸ was carried out replacing Ce by La because of the technical requirement to have even number of f electrons for the calculations. Following the tradition, we report geometrical parameters with an accuracy of 10^{-3} Å and angles with an accuracy of 10^{-1° , although we often discuss the geometrical parameters with lesser accuracy because of the many approximations made in the modeling and in the level of calculation.

Acknowledgment. This work was partially supported by the Director Office of Energy Research Office of Basic Energy Sciences, Chemical Sciences Division of the U.S. Department

of Energy under Contract No DE-AC03-76SF00098. Calculations were in part carried out at the national computing center CINES and CALMIP (France). O.E. thanks the Miller Institute for a Visiting Miller Professorship at U.C. Berkeley. The French authors thank the CNRS and the Ministère of National Education for funding.

Supporting Information Available: Complete list of authors for the Gaussian 98 program in ref 37. List of energies, free energies in au, and coordinates of all calculated systems. This material is available free of charge via the Internet at <http://pubs.acs.org>.

JA0504800

(38) Reed, A. E.; Curtiss, L. A.; Weinhold, F. *Chem. Rev.* **1988**, 88, 899.